

# Design and Analysis of a Compact Dilution Refrigerator

Jacob Higgins

October 24, 2017

## Contents

<b>1</b>	<b>Introduction</b>	<b>3</b>
<b>2</b>	<b>Principle of Operation</b>	<b>4</b>
2.1	$^3\text{He}/^4\text{He}$ Mixtures . . . . .	4
2.2	Individual $^3\text{He}$ and $^4\text{He}$ . . . . .	5
2.3	Enthalpy of Mixing . . . . .	6
2.4	Osmotic Pressure . . . . .	6
<b>3</b>	<b>Parts of the Dilution Refrigerator</b>	<b>7</b>
3.1	The 1 K Pot/Condenser . . . . .	8
3.2	The Still: Cooling Down . . . . .	9
3.3	Heat Exchangers . . . . .	9
3.4	Mixing Chamber . . . . .	10
3.5	The Still: Removing the $^3\text{He}$ . . . . .	10
<b>4</b>	<b>Design of the Insert</b>	<b>11</b>
4.1	Starting Point: The $^4\text{He}$ Cryostat . . . . .	11
4.2	The Proposed Insert . . . . .	11
4.3	Upper Dilution Fridge . . . . .	14
4.3.1	Upper Flange . . . . .	14
4.3.2	Cylinder/1 K Plate . . . . .	15
4.4	Dilution Unit . . . . .	18
4.4.1	Vacuum Jacket . . . . .	22
4.4.2	Pre-cooler/Condensor & Main Impedance . . . . .	23
4.4.3	Still . . . . .	23
4.4.4	Secondary Impedance . . . . .	25
4.4.5	Main Graphite Support . . . . .	26
4.4.6	Heat Exchangers . . . . .	27
4.4.7	Mixing Chamber . . . . .	28

<b>5</b>	<b>Design Analysis</b>	<b>30</b>
5.1	Heat Load of the Mixing Chamber . . . . .	30
5.1.1	Initial Heat Load . . . . .	30
5.1.2	Continuous Heat Leak . . . . .	32
5.1.3	Microwave Heat Load . . . . .	32
5.2	Heat Exchanger Analysis . . . . .	33
5.3	Pressure Profile . . . . .	37
5.3.1	Pressure Gradient Along a Circular Heat Exchanger . . . . .	37
5.3.2	Pertinent Properties of $^3\text{He}$ . . . . .	38
5.3.3	Tracing the Pressure Profile . . . . .	38
<b>6</b>	<b>Conclusion</b>	<b>40</b>
<b>A</b>	<b>Heat Equation for Initial Heat Load</b>	<b>43</b>
A.1	Initial Formulation of the Equation . . . . .	43
A.2	Simplifying the Equation . . . . .	46
A.3	Final Heat-Equation Form . . . . .	47

## Abstract

A design is proposed that would replace the mechanical insert for a pre-existing 1 K helium cryostat with an insert modified for additional dilution refrigeration, the goal of which would be to lower the minimum temperature below 100 mK. This insert is designed such that all dilution components fit with the geometric constraints presented by the cryostat. Schematics and dimensions of the design are given, as well as several analyses of the thermodynamics involved. Due to the cryostat's involvement in dynamic nuclear polarization (DNP) experimentation, special design considerations are examined and possible heat load to the dilution fridge is discussed.

## 1 Introduction

Dilution refrigeration is a technique used to cool down samples to temperatures lower than are achievable by conventional pumping techniques. Since the idea of the dilution refrigerator was first realized by Heinz London in the 1950's, much research, analysis and experimentation has been done on determining its limitations and optimizing its performance. Today, it is a reliable method of reaching low temperatures in a relatively simple manner.

The typical temperature range of dilution fridges is 10 mK to 25 mK, but if designed carefully, temperatures even lower may be achieved. The lowest temperature achieved by a dilution refrigerator was constructed by Frossati et al. [1], producing temperatures of 1.9 mK.

Starting with principle of operation and leading to the actual design, the following paper outlines a proposal for a dilution fridge that will serve as the insert for a  $^4\text{He}$  cryostat already in our possession. The cryostat is used for dynamic nuclear polarization (DNP) experimentation, and cools samples to 1 K through evaporative cooling, pumping on the  $^4\text{He}$  bath surrounding the sample. Once the sample is in thermal equilibrium, the nuclear magnetic resonance (NMR) system is activated, microwaves broadcast on the sample, and the DNP begins. With the proposed dilution fridge insert, however, this bottom temperature is expected to be lowered to under 100 mK – well within the range of typical dilution fridges. At these temperatures, the spin relaxation time will allow the sample to remain polarized once the microwaves are turned off.

For many dilution fridges, it is considered a failure for the minimum achievable temperature to be above 30 mK, so many of the design principles in this paper have been borrowed from authors with this mindset. One major advantage for this project, then, is the simple fact that that goal of achieving minimum temperatures of 100 mK or below is considered for most a dilution fridges a “failure”.

The challenge as it stands is to build such a dilution fridge that can fit and function within the constraints of the existing hardware. The diameter of the insert is approximately 4 cm, and the top of the dilution unit has to reside underneath the 1 K level within the cryostat, allowing a total length of 50 cm. To someone who has ever seen a dilution

refrigerator before, this problem seems insurmountable, since many are considerably larger than those dimensions. Fortunately, though, most of the bulk in a dilution fridge has nothing to do with the dilution at all, instead acting as a preliminary system to bring the temperature down as much as possible using traditional pumping techniques, usually 1 K – precisely the lower temperature of the cryostat. The rest of the fridge, which performs its dilution magic to bring the ambient temperature down even further, has considerably more leeway in terms of designing it. Thus, construction of a dilution fridge unit for the insert of the surrounding cryostat isn't so much as a design challenge, yet more of a natural extension for the system.

Nevertheless, there are still many design aspects of the insert to be worked out. First, though, a basic overview of the principle of operation is described for those unfamiliar with how a dilution fridge works.

## 2 Principle of Operation

### 2.1 $^3\text{He}/^4\text{He}$ Mixtures

The key to any dilution fridge is the use of two helium isotopes:  $^4\text{He}$ , the naturally occurring isotope, and  $^3\text{He}$ , a very rare isotope that can be expensive to buy (currently about \$2100 per liter). For academic use,  $^3\text{He}$  is usually harvested as a bi-product of the radioactive decay of tritium, an isotope of hydrogen. When combined, the resulting mixture has several unique properties at milliKelvin temperatures.

Fig. 1 shows the behavior of such mixtures, with temperature of the mixture on the y-axis and the molar fraction of  $^3\text{He}$  along the x-axis. Three different regions are pictured, only two of which are physically realizable. Because of how these regions appear on the diagram, this is often called lambda line.

As the temperature of a mixture decreases, it moves along a vertical line downward in the figure. Eventually, it will hit a certain forbidden zone, labeled as “unstable composition” in the figure, at which point it will spontaneously separate into two different phases. One phase will be a normal liquid, corresponding to the point that lies on the right side of the lambda line. The other phase will be a superfluid, and have less of a  $^3\text{He}$  concentration than the normal phase. Because the normal liquid is less dense than its superfluid counterpart, it will sit atop the mixture as it separates out, much like oil and water.

Lowering the temperature further, both points along the lambda line move in unison downward. According to the diagram, the normal fluid approaches a state of being 100%  $^3\text{He}$ ; for this reason, this phase is called the *concentrated* phase. On the other side of the lambda line, the  $^3\text{He}$  decreases; this portion is called the *dilute* phase, and is the namesake for the dilution fridge.

One thing to note about the graph is that as the temperature approaches absolute zero, the molar fraction of  $^3\text{He}$  in the dilute phase does not approach zero, as one might expect. Instead, it approaches a finite value, approximately 6.3%. While it may seem a

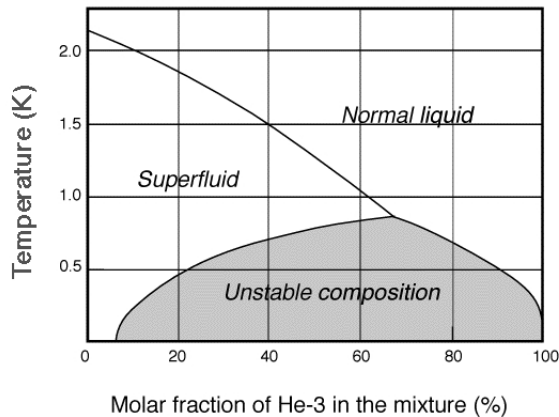


Figure 1: The lambda line for mixtures of  $^3\text{He}/^4\text{He}$ .

subtle point, this is the key feature that gives the dilution fridge its power. In the words of Wheatley, Vilches and Abel, this is what makes the dilution fridge more than just a “scientific curiosity.” [2]

## 2.2 Individual $^3\text{He}$ and $^4\text{He}$

To understand why this happens, consider now the individual atoms of  $^3\text{He}$  and  $^4\text{He}$ . When brought down to these temperatures, both approach and/or pass below their respective Fermi degenerate temperatures, meaning that the quantum mechanical nature of each isotope begins to determine the properties of the substance itself. Since  $^4\text{He}$  is a boson, it follows Einstein-Bose statistics and becomes a fluid that has virtually no viscosity, zero entropy and therefore zero specific heat; a so-called “superfluid.” It is effectively a massive vacuum through which  $^3\text{He}$  atoms may pass through with minimal interaction with the  $^4\text{He}$  atoms.

$^3\text{He}$ , on the other hand, is a fermion, meaning it follows Fermi-Dirac statistics, a mathematical model for particles that obey the Pauli-exclusion principle. It is lighter, has a greater zero-point motion, and generally exhibits a quantum degeneracy pressure when confined to smaller volumes.

Suppose that two containers of pure  $^3\text{He}$  and  $^4\text{He}$  are both cooled to near absolute zero and combined such that, in first moment of contact, the  $^3\text{He}$  rests atop the  $^4\text{He}$  with no motion of the atoms between either mixture. At the boundary where those two phases meet, both the  $^3\text{He}$  and  $^4\text{He}$  have the ability to either remain in their respective phase, or traverse the phase boundary separating the two. Physically, this is determined by which phase has a larger binding energy, according to each particle.

A  $^3\text{He}$  atom will experience van der Waals forces attracting it from either side of the

phase boundary, comparable in strength. But, because the  $^3\text{He}$  atom has a larger zero-point motion than  $^4\text{He}$ , its binding energy will be greater when immersed in liquid  $^4\text{He}$ , so it crosses the phase boundary and enters into the  $^4\text{He}$  phase.

As time passes, more and more  $^3\text{He}$  atoms move in the same direction, increasing the concentration of  $^3\text{He}$  within the  $^4\text{He}$  dilute phase. This causes its binding energy to decrease in the process, due to its Fermi character. Eventually, an equilibrium concentration will be reached such that the binding energies of the  $^3\text{He}$  concentrated phase and the dilute phase are equal.

### 2.3 Enthalpy of Mixing

As mentioned before, there are many systems that rely on vacuum pumping to obtain lower temperatures. As the pressure above a liquid-air boundary is lowered, more high-energy atoms have a chance to jump that boundary from liquid into air, effectively leaving the liquid slightly cooler. This is the same principle as blowing on a hot bowl of soup in the hopes of cooling it faster to eat.

To some degree, the dilution fridge acts as an upside-down bowl of soup that needs to be cooled down. Right where the phase boundary occurs,  $^3\text{He}$  atoms that have enough energy can jump from the concentrated phase to the dilute phase. It is this transition from one phase to another that costs kinetic energy, cooling the phase boundary in the process. Mathematically, this cooling can be tracked through the change in enthalpy of the system. For  $n_3$  moles that pass through the phase boundary, the amount of heat that is absorbed is equal to the difference in the molar enthalpy of  $^3\text{He}$  in the dilute phase, or  $H_d(T)$ , and the molar enthalpy of  $^3\text{He}$  in the concentrated phase, or  $H_c(T)$ , both of which are functions of temperature  $T$ . The rate of heat absorption, or cooling power, then can easily be formulated to be:

$$\dot{Q} = n_3[H_d(T) - H_c(T)] \quad (1)$$

For temperatures under 50 mK (the typical temperature range of the dilution fridge), these enthalpies may be replaced with Eq. (2) [6].

$$\dot{Q} = n_3(96T_M^2 - 12T_N^2) \quad [\text{W}] \quad (2)$$

Here,  $T_M$  is temperature of the dilute phase, and  $T_N$  is the temperature of the incoming  $^3\text{He}$  being supplied to the phase boundary.

### 2.4 Osmotic Pressure

Another critical component to the dilution process is the circulation of  $^3\text{He}$  throughout the entire system. For this to happen,  $^3\text{He}$  must be taken away from the phase boundary so that more  $^3\text{He}$  can make that jump across it, all without moving the superfluid  $^4\text{He}$  through

which it travels. This is achieved through establishing an osmotic pressure gradient along the dilute side of the dilution fridge, biased in such a way that will carry the  $^3\text{He}$  away from the phase boundary.

When an atom of  $^3\text{He}$  floats through the dilute phase of the mixture, it's Fermi character allows it to travel through the superfluid medium with virtually no interaction between and the  $^4\text{He}$  around it. It's motion, then, can effectively be modeled as a Fermi gas traveling through the massive vacuum of superfluid  $^4\text{He}$ . This is the basic model for van't Hoff's law, which says that for  $n$  moles of a substance at temperature  $T$  immersed in a solution of volume  $V$ , the osmotic pressure  $\Pi$  can be found by:

$$\Pi \cong \frac{nRT}{V} \quad (3)$$

This equation may be modified to fit the situation of the dilution refrigerator by replacing the total volume  $V$  with the molar volume  $V_{m,4}$  of  $^4\text{He}$  and  $n$  with the fraction of  $^3\text{He}$  found within the solution. The osmotic pressure difference between the phase boundary (having pressure  $\Pi_{mc}$ ) and elsewhere along the dilute side (having pressure  $\Pi_{st}$ ) may be found to be<sup>1</sup>:

$$\Delta\Pi \cong (x_{mc}T_{mc} - x_{st}T_{st})R/V_{m,4} \quad (4)$$

Here,  $x_{mc}$  may be taken to be the finite solubility of the  $^3\text{He}$ , or 6.5%, and for our purposes  $T_{mc}$  to be estimated around 50mK. Typically,  $T_{st}$  may be controlled to be around 0.7K to optimize partial pressures (discussed later).

The greatest osmotic pressure will occur when  $x_{st}$  approaches zero, which, when using nominal values for  $R$  and  $V_{m,4}$ , results in approximately 100 mbar.

### 3 Parts of the Dilution Refrigerator

Although dilution refrigerators are made in a variety of different ways, each share four main components: the 1 K pot/condensor, the still, the heat exchangers and the mixing chamber. Fig. 2 [2] shows a typical dilution fridge, complete with these four components, as well as additional components (impedances, helium bath, etc.) that aid in performance. As  $^3\text{He}$  circulates through the dilution refrigerator, it encounters each of these components at different stages of its cycle, either absorbing or releasing heat in the process.

What follows is a brief description of each component of the dilution refrigerator.

---

<sup>1</sup>The indices  $mc$  and  $st$  aren't arbitrary, and correspond to specific parts in the dilution refrigerator. These will be discussed soon.

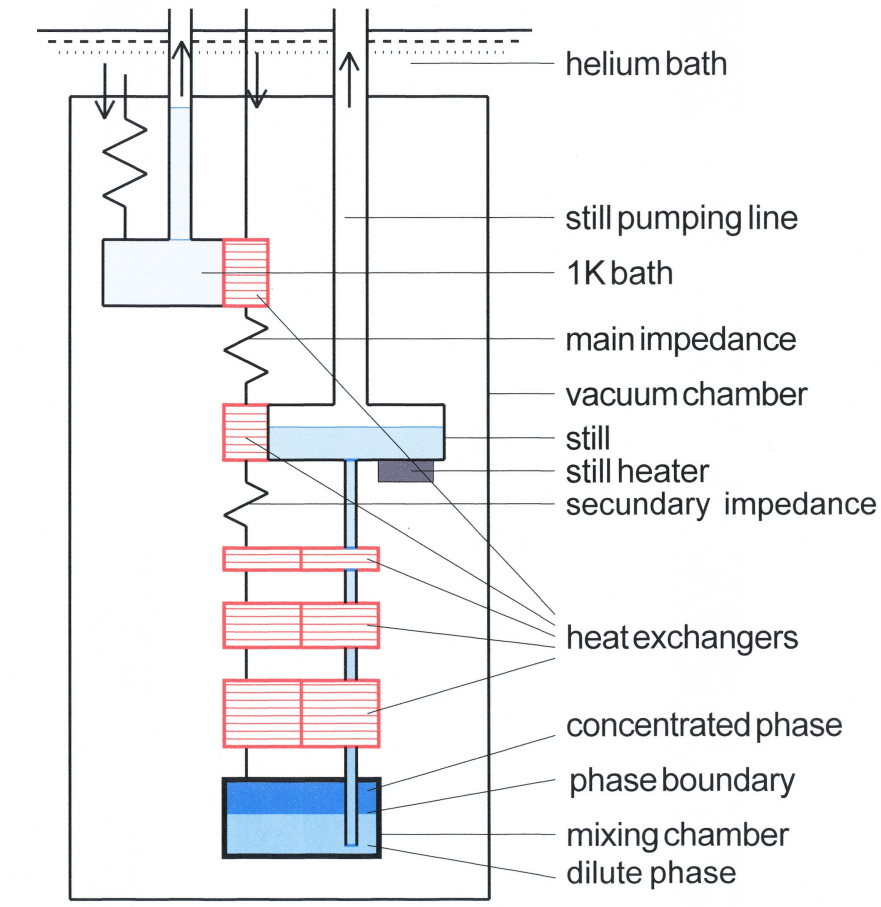


Figure 2: A typical dilution refrigerator.  $^3\text{He}$  is pumped down from room temperature through the various components of the fridge. The arrows show the flow of the  $^3\text{He}$  from component to component. In the diagram, the left side of the dilution fridge is dedicated to cooling the  $^3\text{He}$  as it travels down towards the mixing chamber. Once the  $^3\text{He}$  has crossed the phase boundary of the mixing chamber, it travels upwards (pictured as the right side), where it helps cool the incoming  $^3\text{He}$ .

### 3.1 The 1 K Pot/Condenser

Before  $^3\text{He}$  may be introduced to the cooling system, a temperature of 1 K must first be obtained. This is done through pumping on  $^4\text{He}$ , and involves no “dilution” process before this step. The 1 K pot, then, refers to the final product of cooling via pumping, which is simply a container, or “pot”, of  $^4\text{He}$  that is resting at temperature of approximately 1 K.

It is at this stage that  $^3\text{He}$  now begins its journey through the dilution process. From room temperature, gaseous  $^3\text{He}$  is introduced into the system and is cooled as it travels down into the heart of the refrigerator towards the 1 K pot. Once it arrives and cools down



to 1 K itself, it may now be condensed into a liquid. This is usually achieved through an impedance that increases the pressure of the  $^3\text{He}$  at this particular point in the dilution fridge. If the impedance is engineered in a such way to produce a pressure that is greater than or equal to the vapor of pressure of  $^3\text{He}$  at 1 K, then condensation will occur.

### 3.2 The Still: Cooling Down

Leaving the condenser, liquid  $^3\text{He}$  next travels to the still, which serves several important functions.

The still is a simple cylinder that holds the dilute-phase  $^4\text{He}$  towards which the circulating  $^3\text{He}$  ultimately travels. The  $^3\text{He}$  travels through a continuous heat exchanger that is immersed in this liquid  $^4\text{He}$ , held at about 0.7 K. Enough length of tube is provided so that the  $^3\text{He}$  is cooled to this temperature as well.

After this, the  $^3\text{He}$  then leaves this cylinder and is sent to a secondary impedance. The purpose for this is to maintain a suitable pressure in the still, preventing any liquid  $^3\text{He}$  from evaporating.

### 3.3 Heat Exchangers

Next, the  $^3\text{He}$  then travels through a series of heat exchangers in which the  $^3\text{He}$  is cooled by the dilute phase. On most dilution fridges, there are two main types of heat exchangers that are used: continuous and step. As the names imply, the former produces a smooth temperature gradient along which heat is exchanged, while the latter does the same in discrete steps.

One example of a common continuous heat exchanger is the tube-in-tube, countercurrent heat exchanger. Construction simply consists of fitting one smaller tube inside of a larger tube. Liquid  $^3\text{He}$  is sent downward through the inner tube while the cooler dilute phase fills the annular space. This is usually put in place immediately after the still.

The step exchangers, on the other hand, are containers that are separated into two large compartments, one for the concentrated phase and another for the dilute phase. Filling each compartment is sintered metal, such as copper, which greatly increases the amount of surface area with which both liquids are in contact. The main purpose for this (and these types of exchangers) is to overcome the Kapitza thermal resistance<sup>2</sup> that presents itself at low temperatures, and are usually used when trying to obtain the lowest possible temperatures for the dilution fridge.

Having an effective heat exchanger is invaluable to the performance of a dilution fridge. To see this, consider Eq. 2 in the case of no cooling power, or  $\dot{Q} = 0$ . Rearranging terms,

---

<sup>2</sup>This refers to the resistance of heat to flow across the interface of two different substances. In the case of dilution refrigeration, the interface is usually the boundary between liquid Helium and the metal of a heat exchanger. Because of this inherent resistance along interfaces, increasing the surface area of the interface is the most effective method of reducing this resistance.

this is achieved when the incoming  $^3\text{He}$  has a temperature only three times greater than that of the dilute solution. This means that the condition for *any* cooling to take place must satisfy  $T_N/T_M \leq 3$ . This stresses the importance of proper heat exchange, as a dilution fridge whose mixing chamber has a temperature 50 mK must cool its incoming  $^3\text{He}$  from 0.7 K down to at least 150 mK for cooling to happen.

### 3.4 Mixing Chamber

The mixing chamber is where the cooling power of the dilution refrigerator lies. After exiting the series of heat exchangers above,  $^3\text{He}$  then enters into the mixing chamber. Here, the incoming  $^3\text{He}$  is sent to the concentrated phase, sitting atop the dilute phase. By an osmotic pressure gradient created at the still,  $^3\text{He}$  in the dilute side is moved away from the phase boundary. This in turn lowers the local binding energy of the dilute phase at the phase boundary, inviting more  $^3\text{He}$  atoms to leave the concentrated phase and transition into the dilute phase, producing the desired cooling effect.

### 3.5 The Still: Removing the $^3\text{He}$

Osmotic pressure pushes the  $^3\text{He}$  from the mixing chamber, through the heat exchangers and eventually back to the still, instead this time the  $^3\text{He}$  rests in the dilute phase. New  $^3\text{He}$  incoming into the system is sent through a small tube, which is immersed in this dilute phase, cooling the incoming  $^3\text{He}$ .

The entire volume of the still isn't filled with this dilute phase however, and quite a bit of volume is dedicated to  $^3\text{He}/^4\text{He}$  vapor. Connected to the top of the still is a tube that leads directly outside the refrigerator to a pump that removes this  $^3\text{He}/^4\text{He}$  vapor, in turn allowing more vapor to be produced from the liquid dilute mixture below it. As more  $^3\text{He}$  turns back into a gaseous vapor, less is left in the dilute phase at the vapor-liquid boundary. This difference in  $^3\text{He}$  concentration from the mixing chamber to the still is what creates the osmotic pressure difference that drives the  $^3\text{He}$  throughout the entire dilute phase.

The vapor pressure must be high enough to allow a reasonable flow rate of  $^3\text{He}$  through the fridge, which is achieved at temperatures higher than what the still naturally settles in steady-state operation. For this reason it is often the case that heat must be artificially given to the still in order to raise its temperature, thus raising the vapor pressure above it.

At the same time, though, the partial pressure of  $^4\text{He}$  also rises with temperature. In practice, it is beneficial to the performance of the dilution fridge to reduce the amount of  $^4\text{He}$  that is circulated through the system, as more  $^4\text{He}$  going into what is supposed to be 100%  $^3\text{He}$  means greater temperature gradient instabilities, as well as a greater heat load to the heat exchangers. The challenge, then, is to optimize the total pressure while at the same time minimizing the partial pressure of the  $^4\text{He}$ . This optimal temperature has been found to be around 0.7 K [3].

Since  $^4\text{He}$  is a superfluid at these temperatures, another concern to be cognizant of is

$^4\text{He}$  film flow up the sides of the inner wall of the still. Without taking any precaution against this, this provides another avenue for large amounts of  $^4\text{He}$  to enter into circulation. One effective solution is a film suppressor that stops the thin  $^4\text{He}$  film from creeping up the sides of the still and evaporating/being pumped out with the  $^3\text{He}$ .

## 4 Design of the Insert

In this section, a design is put forth that is believed will reach the target temperature of under 100 mK while remaining within the geometric constraints presented by the existing cryostat, described below. The next section (Sect. 5) is concerned with the mathematical analysis of several key design aspects.

### 4.1 Starting Point: The $^4\text{He}$ Cryostat

The starting point for design was the pre-existing  $^4\text{He}$  cryostat, pictured in Fig. 3.

Encasing the entire system is the metal chamber, which enables the creation of an inner vacuum jacket, protecting the inner components from the heat leak of the surrounding atmosphere. The first step towards cryogenic temperatures is the liquid nitrogen, which rests at about 77 K. Further towards the center is a large chamber that holds liquid  $^4\text{He}$  at 4 K (this helium is purchased and transferred into the dewar). Inside a smaller chamber at the geometric center of the dewar, a large evaporation pumping system cools the  $^4\text{He}$  down to 1 K.

The 1 K heart of the dilution refrigerator is reachable by use of an insert, which is placed into the cryostat through an opening on the top. The insert itself is approximately one meter in length, and the separator (labeled in the diagram, the point below which the 1 K helium begins) is approximately 50 cm from the bottom of the cryostat. With this current setup, the sample used in experiment is placed at the very end of insert and the insert is placed into the cryostat, immersing the sample into the 1 K helium. Microwaves are broadcast to the sample via an NMR line that travels down the middle of the insert and through a horn that amplifies the signal, and DNP begins.

The following design aims to replace the purely mechanical nature of the insert with dilution machinery, enabling a lower temperature to be achieved for experimentation.

### 4.2 The Proposed Insert

The entire dilution insert, shown in Fig. 4, is approximately 1.5 m in length. From the top of the insert down approximately 60 cm (where it reaches the separator inside the cryostat), the proposed dilution insert is very much like the existing insert geometry, and its design has little impact on the dilution process. Mechanically, it must support all components located below it, which has a total weight of about 1 kg, more than manageable by the tensile strength of the usual insert. Below the separator, there is 50 cm of 1 K helium, the

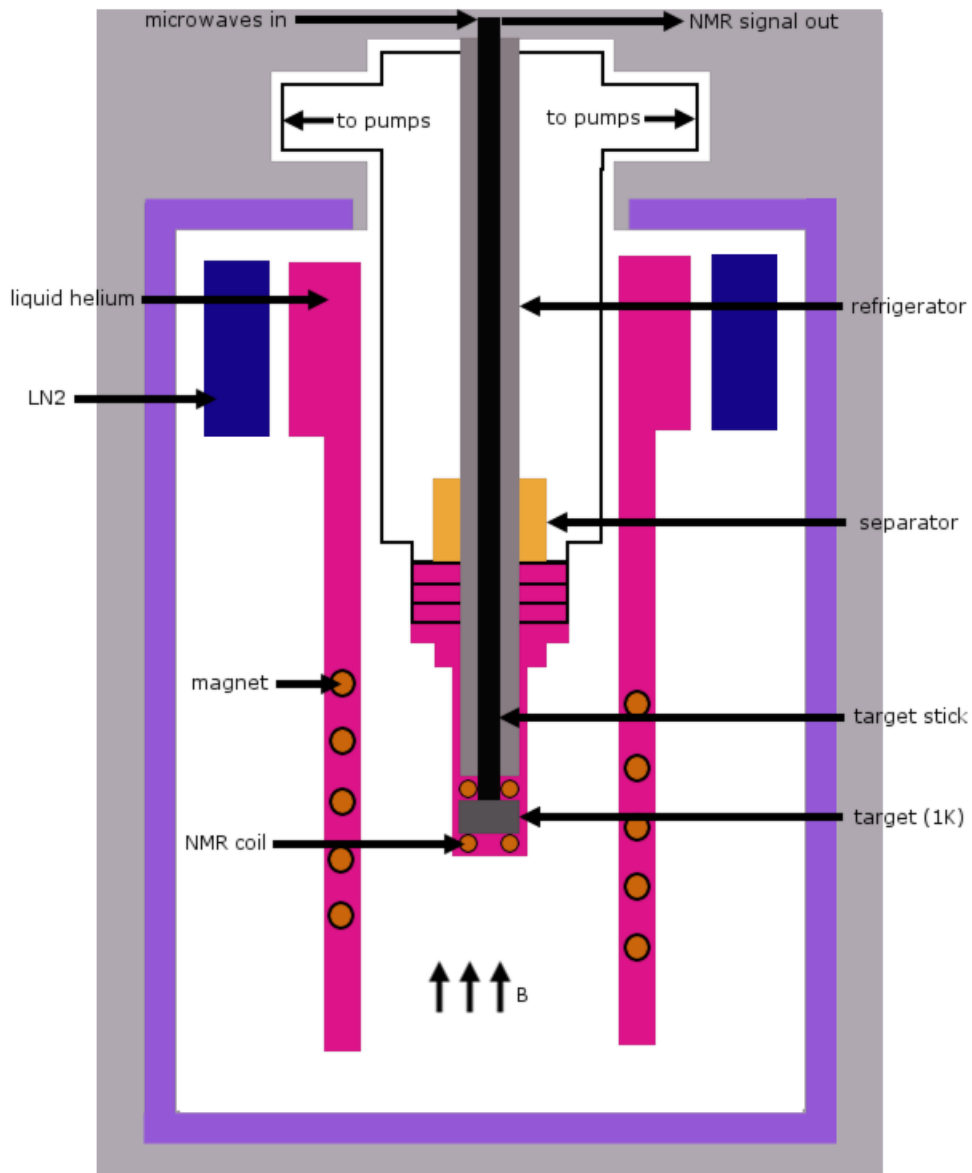


Figure 3: Schematic of the Cryostat. The color scheme is as follows: purple=metal casing, white=inner vacuum jacket, dark blue=liquid nitrogen, magenta=liquid helium, black=insert.

lower 26 cm of which is dedicated to the dilution unit. Between the dilution unit and the separator is a heat exchanger to help pre-cool the  $^3\text{He}$  as it is pumped towards the dilution

unit before reaching the condenser. Again, this pre-cooling heat exchanger is more of a precautionary measure to ensure an adequate condensing rate of the gaseous  $^3\text{He}$  when first entering the fridge, and its exact design has little impact on overall performance. The design of the non-dilution components are discussed in Sect. 4.3, and the dilution unit is discussed in Sect. 4.4.

It should be noted that due to the nature of the experiment, the material used to construct the fridge is 316 L stainless steel (unless otherwise specified for specific components). This particular steel has a low magnetic susceptibility, and thus mechanical components won't interfere with the DNP process.

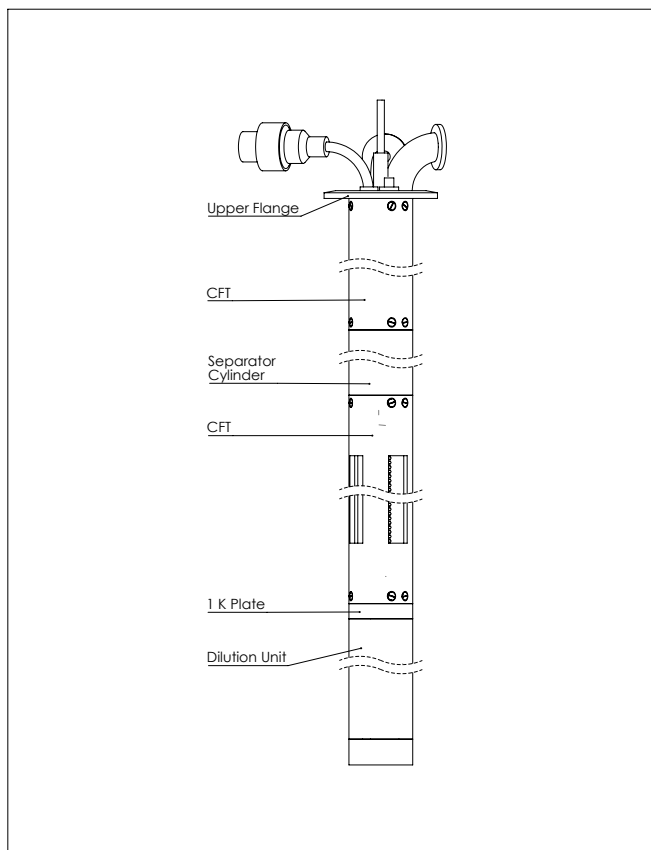


Figure 4: The insert proposed in this paper. It is inserted dilution unit first, so that the upper flange holds the rest of the components up. Carbon fiber tubings (CFT) mechanically connect the flange to the separator cylinder and the dilution unit. Inside the CFT's run electronics, NMR line,  $^3\text{He}$  in and outflow, vacuum line and microwave line.

### 4.3 Upper Dilution Fridge

Supporting the entire dilution unit while inside the  $^4\text{He}$  cryostat is the upper flange (Sect. 4.3.1). Through the upper flange runs the NMR line, microwave line, inner vacuum line,  $^3\text{He}$  in and out lines, as well as a line for electronics inside the fridge.

Midway down the insert is the separator cylinder, below which the cooled  $^4\text{He}$  is deposited. Further down the unit is the 1 K plate, acting as a thermal barrier between the cooler (dilution) components below and the warmer components above. Carbon fiber tubing mechanically connects the cylinder to the upper flange, as well as the 1 K plate to the cylinder. Within this tubing runs all major lines down to the dilution unit.

#### 4.3.1 Upper Flange

The upper flange is made of stainless steel, 7.5 cm in diameter and 5 mm in thickness, it connects hermetically to the cryostat via a KF 50 vacuum clamp. As mentioned before, all components needing to reach within the insert must pass through upper flange, meaning space must be used wisely in order for all components to fit and remain functional (Fig. 5).

On the bottom side of the upper flange (Fig. 6) is a 5.2 cm outer-diameter (o.d.) groove in which a 2 mm thick gasket sits, used to create the hermetic seal. Also on the bottom is a 3.88 cm o.d. metal lip with six M3-threaded holes. Fitted over this lip is a carbon-fiber tube (CFT) that also has six M3-sized sunken screw holes so that machine screws of the same size and type may secure the CFT to the upper flange. In addition to fitting all tubing components onto the upper flange, care was also taken to avoid components touching any screw within the assembly.

Some tubings are larger above the upper flange than below since tubings must be sturdy enough to allow for piping connectors. Both the  $^3\text{He}$  out line and vacuum line connect to their respective pumping systems with a KF 25 vacuum clamp, although before the connection the  $^3\text{He}$  out line has a much larger diameter tubing than the vacuum line in order to maximize the  $^3\text{He}$  pump out power (where it is needed). The  $^3\text{He}$  in line connects to a swagelok VCR metal gasket, and the microwave line has a 9.5 mm outer casing that is included for its stability at the upper flange. Moving from above to below the upper flange, the  $^3\text{He}$  in line reduces in o.d. from 12 mm to 1.6 mm, the  $^3\text{He}$  out line reduces in o.d. from 19 mm to 9.6 mm, and the vacuum line and microwave line remain 7.5 mm and 4.75 mm, respectively.

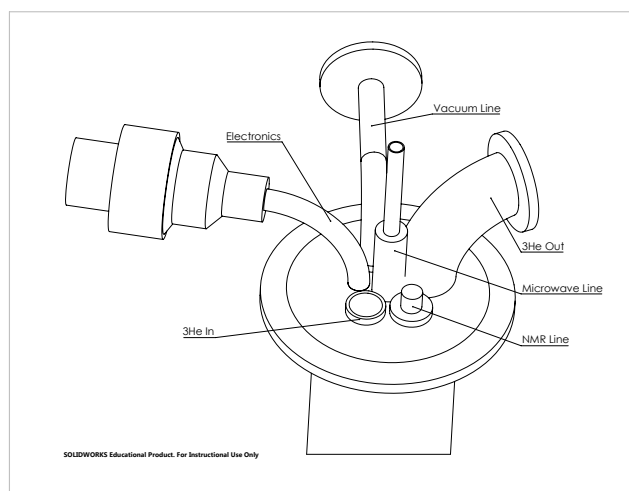


Figure 5: Top-angle view of the upper flange. This view shows the various components that run through the upper flange. Placement was designed so that each component would fit within the limit presented by the KF gasket, avoid the screws attaching the upper flange to the CFT below and optimize convenience near the 1 K plate (e.g. allow room for the pre-cooling heat exchanger).

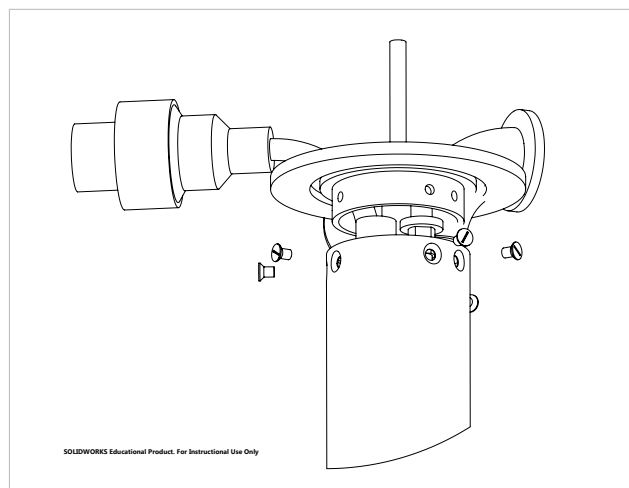


Figure 6: In this view, components are exploded to show how the insert is assembled. The CFT fits over a lip on the upper flange. Sunken M3-sized machine screws are connected through the holes on the CFT to the threaded holes of the upper flange, securing both components in place.

### 4.3.2 Cylinder/1 K Plate

A CFT connects to both the upper and lower portion of the separator cylinder in a similar fashion as the upper flange (see Fig. 7). Each line through the cylinder remains in a similar location as the upper flange.

The CFT below the separator cylinder has sections carved out so that the 1 K  $^4\text{He}$  from the separator will submerge the components within the tubing. In this section, the  $^3\text{He}$  in line will spiral around the microwave line at the center as it descends to the 1 K plate, over a total length of 2.5 m. This maximizes the amount pre-cooling that the incoming  $^3\text{He}$  experiences, allowing it to condense as much as possible before reaching the 1 K plate. The CFT below the separator also connects to the top of the 1 K plate, in the same fashion as before. Fig. 8 shows these features between the separator cylinder and the 1 K plate.



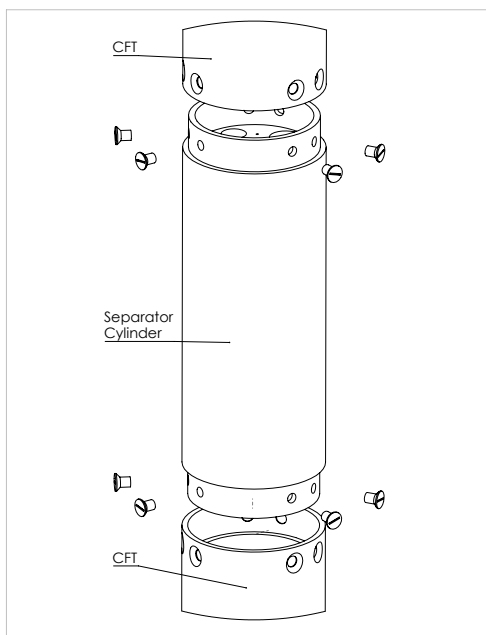


Figure 7: Exploded view of the CFT's fitting to the separator cylinder (inner piping is hidden for clarity).

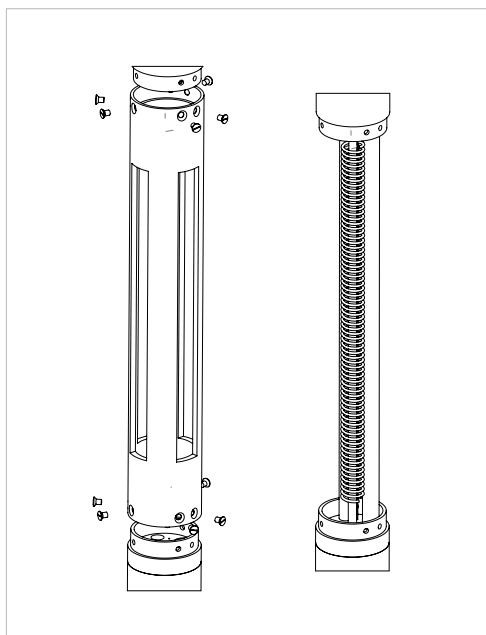


Figure 8: View of the region between the separator cylinder and the 1 K plate, with and without the CFT (left and right, respectively). In the left image, the carved-out section of the CFT may be seen. This is to allow 1 K  $^4\text{He}$  from the separator to cool the inner tubing. In the right image, a spiraling  $^3\text{He}$  in line is shown. This increase in tube length helps pre-cool and condense the incoming  $^3\text{He}$ .

## 4.4 Dilution Unit

Below the 1K plate are the dilution components of the insert. Fig. 9 and 10 show the dilution unit with certain components removed in order to reveal a more comprehensive assembly. Fig. 11 shows the dilution unit with all components.

A vacuum jacket fits around the inner components of the fridge, making no direct contact. The design of this jacket is described in Sec. 4.4.1. Inside the vacuum jacket, a vacuum is established to thermally isolate the inner components of the fridge, preventing heat leaks from effecting the performance of the fridge. This vacuum is established by the vacuum line that runs from the upper flange and terminates at the 1 K plate (see Fig. 12).

The 1 K plate serves as the thermal anchor for the rest of the fridge as it makes contact with the surrounding 1 K helium. Below the 1 K plate is the still, main heat exchanger and mixing chamber, whose functions are described in Sect. 3. A graphite support connects the still to the 1 K plate, while the main graphite support connects the still to the mixing chamber. The main heat exchanger is chosen to be a tube-in-tube, counter-current continuous heat exchanger, the design of which is discussed in Sect. 4.4.6.

The NMR line penetrates the 1 K plate and still, and travels down toward the mixing chamber. Direct contact between the NMR line and the mixing chamber is prevented by the proposal of a “crystal window” atop the mixing chamber, allowing the microwaves to pass through to the sample (inside the mixing chamber, the coldest part of the fridge) without directly touching the mixing chamber. This crystal window and mixing chamber geometry is described in Sect. 4.4.7.

From the top of the 1 K plate to the bottom of the vacuum jacket, the dilution unit is 26.3 cm in length with a diameter of 4.22 cm (including the vacuum jacket).

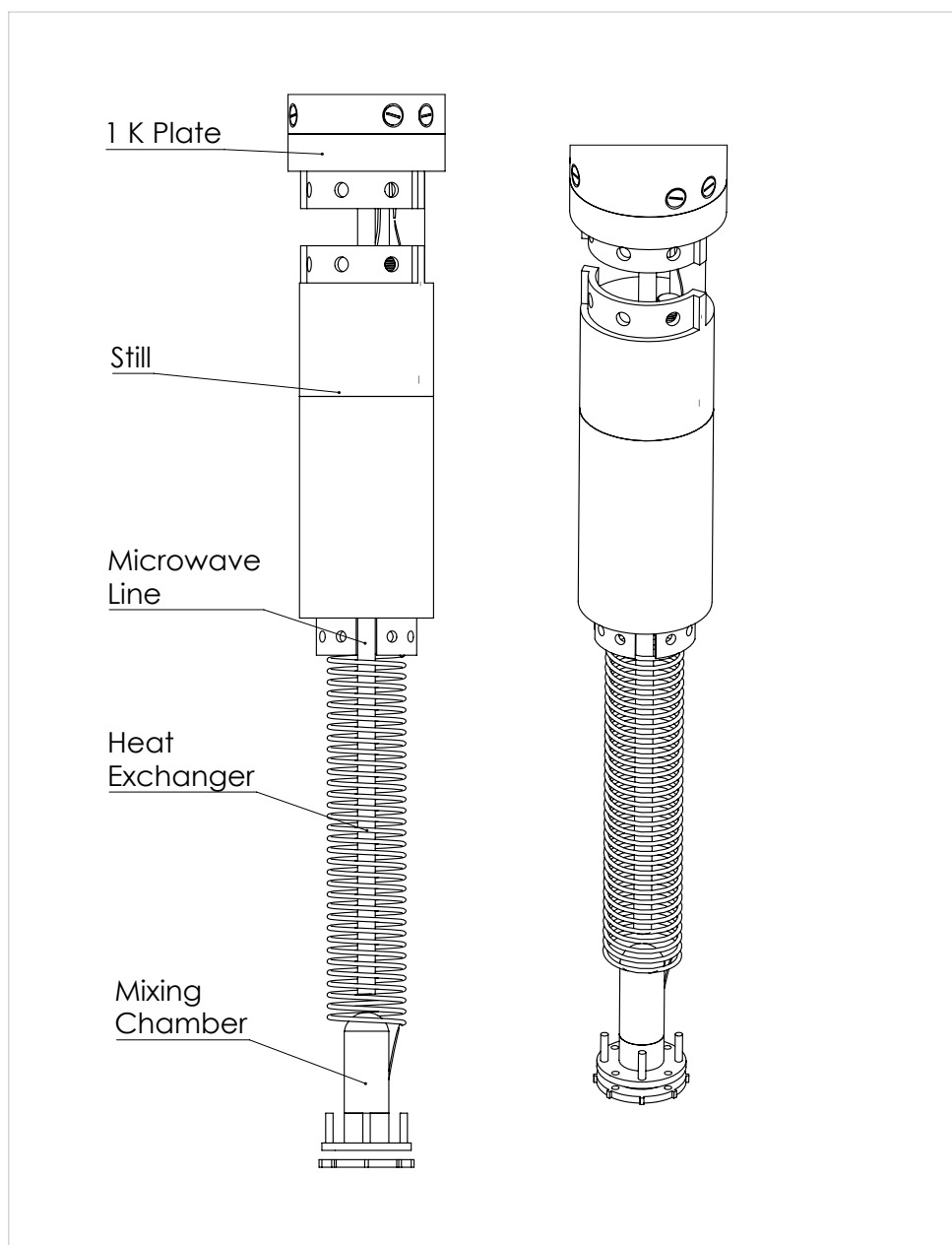


Figure 9: Dilution unit of the proposed insert. Shown are the 1 K Plate, the graphite connection between the 1 K and the still, the still, the main heat exchanger, and the mixing chamber. As can be seen, the main heat exchanger spirals around the NMR line that penetrates down the middle of the insert, terminating at a horn where the microwaves are amplitude and broadcast into the mixing chamber through the crystal window (not shown). Not included in this figure is the graphite support between the still and the mixing chamber, as well as the vacuum jacket.

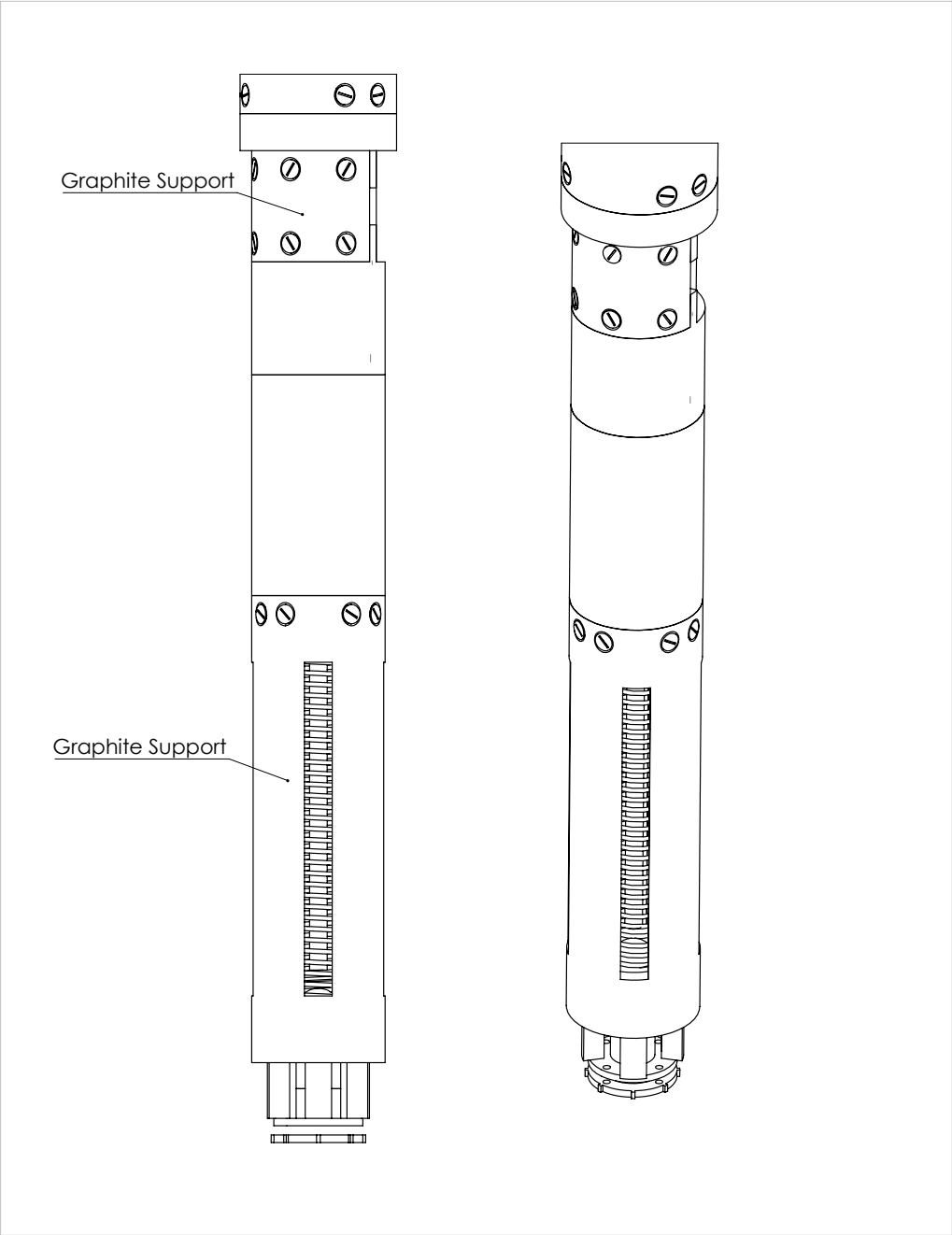


Figure 10: Dilution unit of the proposed insert, including the graphite support between still and mixing chamber. The graphite support between 1 K plate and still is not entirely circular, due to size constraints. The support between still and mixing chamber connects to the bottom of the still in the same manner as the CTF's above the dilution unit (see Sect. 4.3.1). Sections are cut out of the tube so that a vacuum may also thermally isolate the heat exchanger.

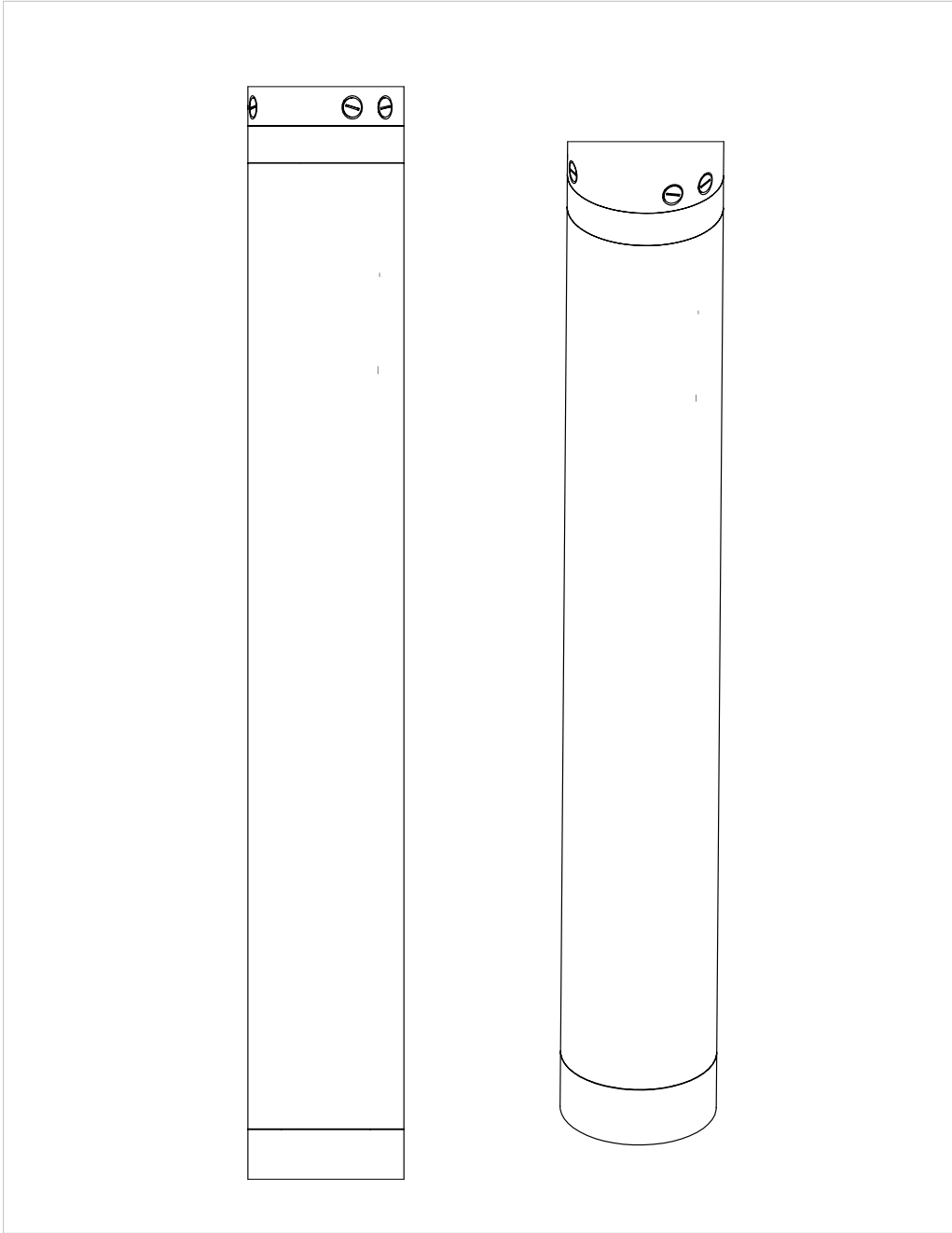


Figure 11: Dilution unit of the proposed insert, with vacuum jacket. A metal jacket is placed around the innards of a fridge to allow for the creation of a vacuum within, thermally isolating those components. A cap is placed at the bottom of the insert to allow access to the mixing chamber.

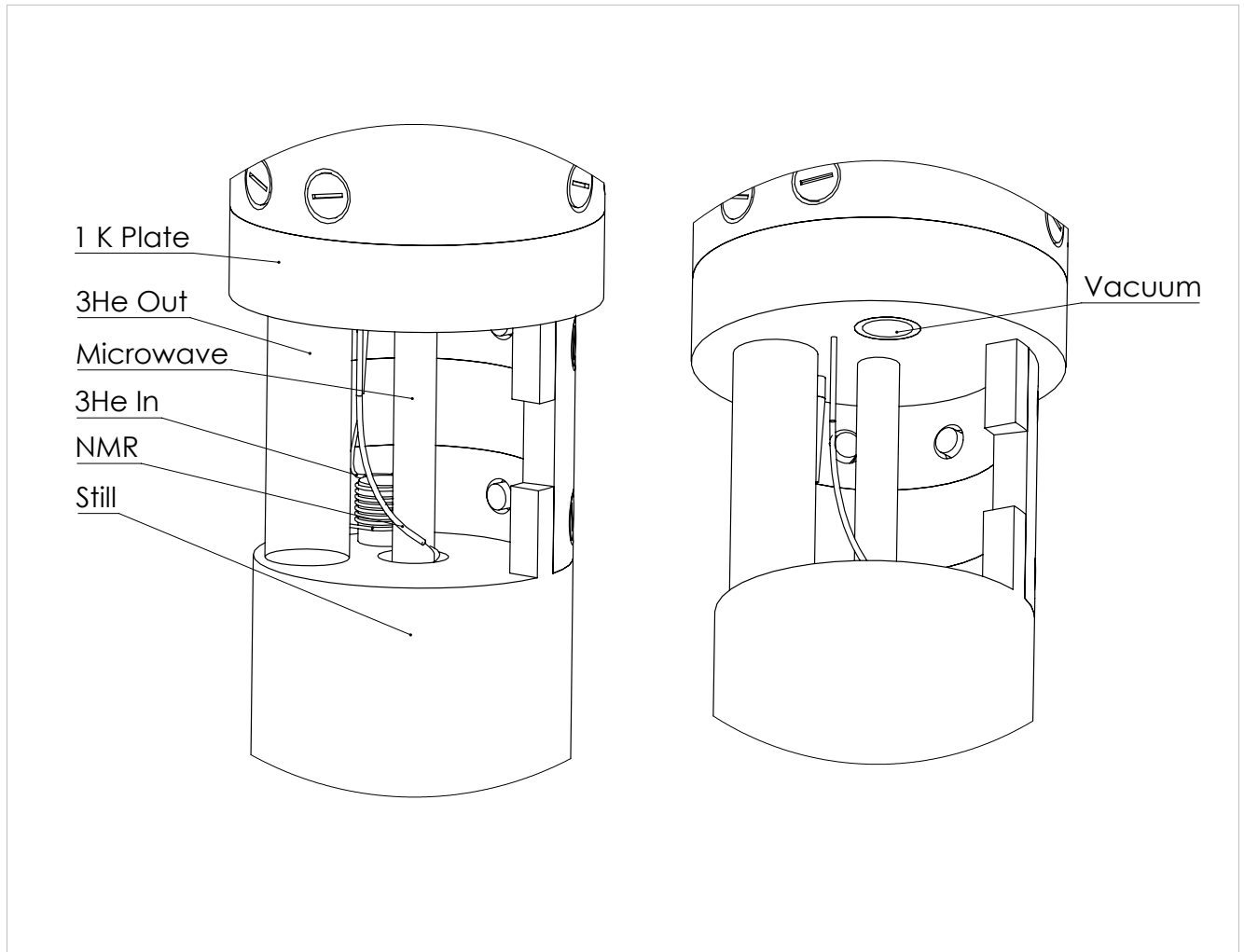


Figure 12: View of the area between the 1 K plate and the still.

#### 4.4.1 Vacuum Jacket

The vacuum jacket that encases the components of the dilution unit will likely be made of the steel, and is comprised of two parts. The first is noted as the main jacket, attached at the 1 K plate and surrounding all of the components (see Fig. 13). It is 0.6 mm in thickness (enough to withstand a 2 atm pressure differential without buckling) and is separated from the innards of the by at least 2.5 mm at any point along its height.

The second is the vacuum jacket cap at the bottom of the dilution unit. While the main jacket is attached to the 1 K plate, the vacuum jacket cap is completely detachable, allowing easy access to the mixing chamber when load/unloading samples.

Where the cap attaches to the main jacket, both have a 2 mm diameter divot into which a ring of indium will be placed, and a number of 2 mm screws holes to attached the cap to the main jacket. The indium is provided in order to create a hermetic seal between the two parts, supporting a high-vacuum environment within the dilution unit.

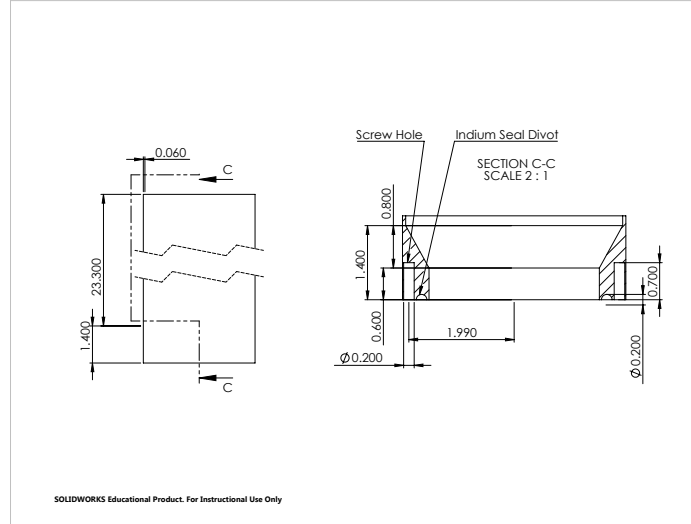


Figure 13: Main vacuum jacket, surrounding the inner components of the dilution fridge.

#### 4.4.2 Pre-cooler/Condensor & Main Impedance

As mentioned before, the incoming  $^3\text{He}$  runs through about 2.5 m of tubing held at 1 K in order to pre-cool/condense the  $^3\text{He}$  as it approaches the dilution unit (Sect. 4.3.2). In order for  $^3\text{He}$  to condense, the gas must be held at a high-enough pressure. For a pre-cooler held at about 1 K,  $^3\text{He}$  may condense in a pressure range of 25-200 torr [17]. The main impedance immediately follows the pre-cooler on the  $^3\text{He}$  in line, and is the component that both creates the pressure needed to condense the  $^3\text{He}$  as well as control the molar flow rate. It is desired for the molar flow rate (the rate at which liquid  $^3\text{He}$  leaves the condenser) to be less than the rate at which the condenser actually condenses, the reason being that if  $^3\text{He}$  leaves the condenser faster than it builds up, there will be moments in time that the condenser is empty, enabling gaseous  $^3\text{He}$  to pass through into circulation. This adds onto the heat load of the still, as well as possibly warming up the heat exchangers [4].

#### 4.4.3 Still

The still is cylindrical in shape, with the exception of a section along the axis of the cylinder that does not commute with the inside of the still, creating an annular space for the dilute

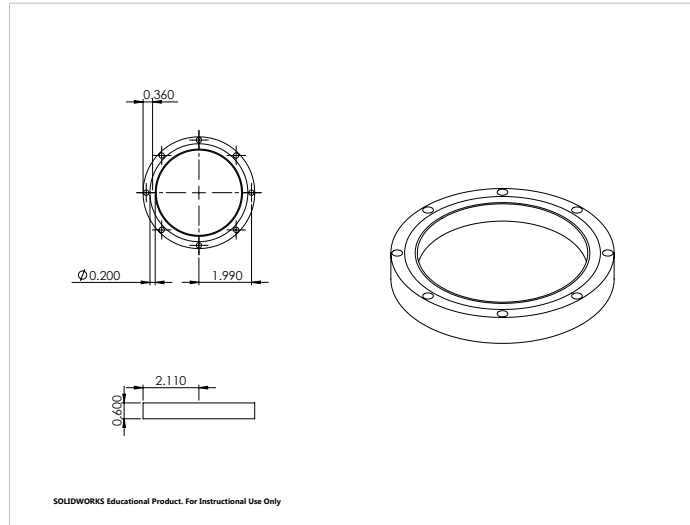


Figure 14: Vacuum jacket cap.

$^3\text{He}$  (Fig. 15). This allows the microwave line to run down to the mixing chamber without coming in contact with the still (the NMR line is also wrapped around the microwave line as it runs down). The still has an o.d. of 3.6 cm, and inner diameter (i.d.) of 8 mm, with 0.5 mm thick walls. Both the  $^3\text{He}$  out line and the  $^3\text{He}$  in line are connected to the annular space of the cylinder through the top of the still (see Fig. 12).

In designing the still, Frossati (1978) explains that there are two main points to keep in mind. First is that the free surface area of the liquid  $^4\text{He}$  on the dilute side must be large enough to facilitate an appropriate amount of evaporation. This is especially concerning in this situation, for the free surface area is not something controllable in the least, but is a design constraint of the insert itself. Given a liquid  $^4\text{He}$  surface of 4 cm in diameter, the resulting surface area would then be  $13\text{ cm}^2$ . To this, Frossati only briefly comments that, for a molar flow rate of  $10^{-4}$  moles/sec, a surface area of  $10\text{ cm}^2$  would be good enough.

Secondly, Frossati explains that the still must also prevent the circulation of  $^4\text{He}$ , which (as explained in Sect. 3.5) tends to crawl up the surfaces of the container in the form of a super-fluid film. This is prevented by the inclusion of a super-fluid film suppressor, which is simply a sharp edge over which the superfluid cannot travel (due to the jagged nature of the path). Two sharp edges must be included, since the annular space in which the dilute side sits has two inner surfaces. For ease of construction, the still is initially set as two different pieces. The two film suppressors are inserted into one of the pieces, and the other piece is placed over them and welded to the first piece, securing the film suppressors inside.

Finally within the still is the  $\text{He}^3$  heat exchanger that cools the incoming, newly condensed  $\text{He}^3$  to 0.7 K. Again borrowing from Wheatly, Rapp and Johnson, cupronickel



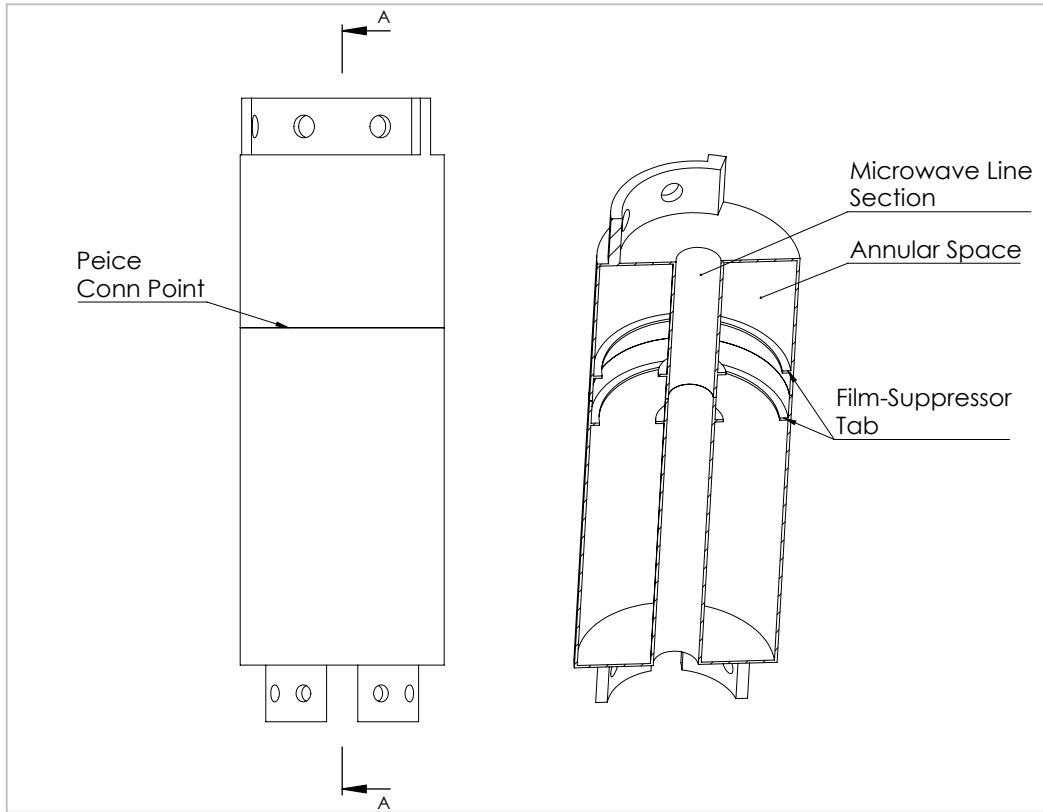


Figure 15: Cross-section of the still, showing the section for the microwave line and the annular space for the dilute liquid. Also shown are the tabs on which the film suppressors are supported within the still, as well as the location of the connection between the two still pieces.

tubing of 0.4 mm outer diameter and 0.08 thickness was used, with a total of 150 cm of length submerged in the liquid  $\text{He}^4$ . This length of tubing is easily compact within the still space.

#### 4.4.4 Secondary Impedance

As the  $^3\text{He}$  passes through the heat exchangers within the still, the pressure at which it passes should remain considerably above vapor pressure, lest any  $^3\text{He}$  re-evaporate and add a greater heat load to the system. To avoid this, it is common practice to add a secondary impedance immediately below the still, allowing pressure in the still to remain above vapor pressure. It is important to place the secondary impedance in the highest possible temperature ranges to prevent any viscous heating affects.

The pressure drop across the impedance itself should be low, to lessen any heating affects due to the isenthalpic expansion of the liquid  $^3\text{He}$ . At these low temperatures,

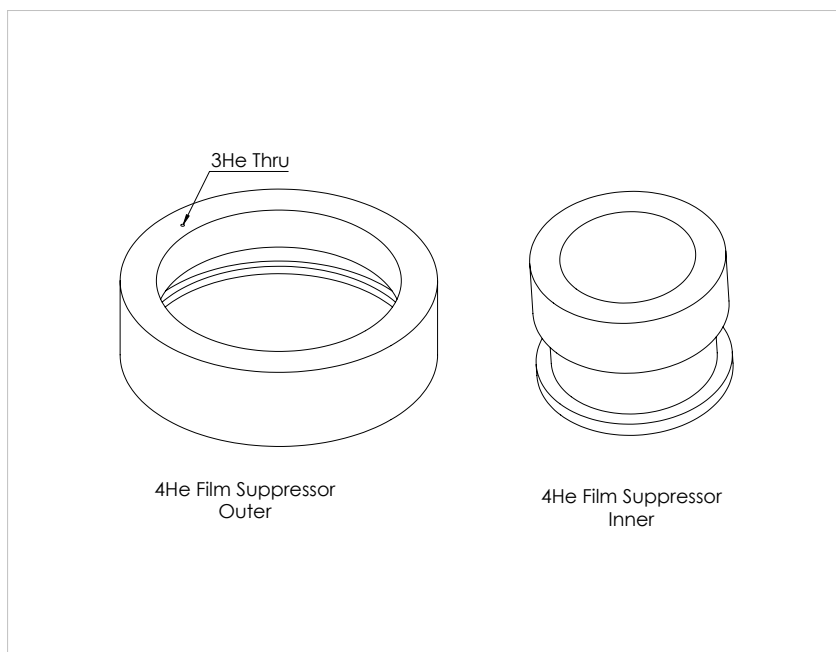


Figure 16: Film suppressor located within the outer and inner annular surfaces of the still. Noted on the outer film suppressor is a hole through which the  $^3\text{He}$  in line passes (so it itself won't provide a surface up which  $^4\text{He}$  may crawl).

this rise in temperature is approximately proportional to the molar volume of the  $^3\text{He}$  and inversely proportional to the molar specific heat:  $(\partial T/\partial P)_H \approx -v_3/c_p$ . Radebaugh and Siegwarth [4] give this value to be -1.3 mK/torr at 0.7K, which they assert increases substantially the lower the temperature.

To this end, they suggest that the pressure drop be 10 torr – this conservatively allows the temperature in the still to be as high as 1 K before re-evaporation occurs, while raising the temperature of the concentrated phase an approximate 13 mK.

To create this impedance, a short length of bare manganin wire can be inserted into the  $^3\text{He}$ -carrying, cupronickel tubing. Before construction, the impedance value can be tested and adjusted to allow for the desired pressure drop for the correct molar flow rate.

#### 4.4.5 Main Graphite Support

Connecting the still and the mixing chamber is a tube of length 12.6 cm, outer diameter 3.6 cm and inner diameter 2.75 cm. This tube fits around the bottom of the still and attaches to it via eight M3 machine screws. This design of the support provides stability and simplicity as it both secures the mixing chamber and allows room for the NMR line at the center of the unit. It also provides mechanical support for the microwave line, since

the microwave line isn't connected to the still itself (in other words, the microwave line runs from the 1 K plate to the main graphite support without touching the still).

The material chosen for the main support is pitch-bonded graphite, suggested by Wheatley, Vilches and Abel [2]. This material is unique because it is a good thermal conductor at higher (room) temperatures and becomes a poor thermal conductor at lower (cryogenic) temperatures, i.e. it acts as passive heat switch. This allows quick-cooling when the dilution process first begins and the innards are still room temperature, and prevents a big heat load to the mixing chamber during steady-state operation.

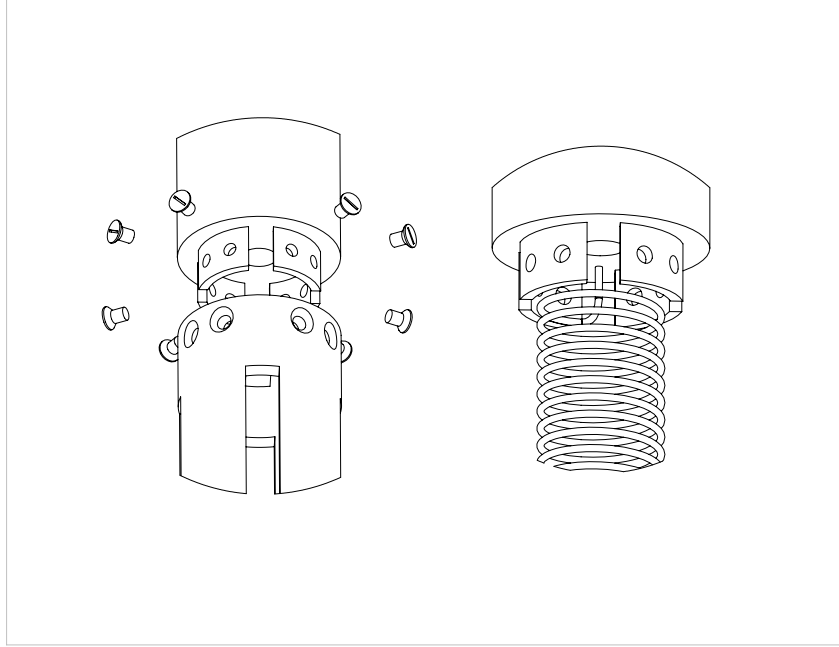


Figure 17: View of the area below the still. The image on the left shows how the main graphite support connects to the bottom of the still, while the image to the right the main heat exchanger spiraling down to the mixing chamber (graphite support hidden).

#### 4.4.6 Heat Exchangers

The main heat exchanger of the proposed dilution insert is a tube-in-tube, counter-current continuous heat exchanger 200 cm in length. Modeled after one built and tested by Wheatly, Rapp and Johnson [11], the tube is comprised of a 70% copper and 30% nickel alloy. The outer tube will have an outer diameter of 1.19 mm and inner diameter of 1.03 mm, while the inner tube will have an outer diameter of 0.4 mm and inner diameter of 0.24 mm. The inner tube will carry the incoming  $^3\text{He}$  towards the mixing chamber, while the annular space between the tubes will house the dilute phase that runs up to the still.

This particular design was chosen for two reasons. First and foremost, the simplicity of tube design allows for both compactness and ease of construction. Despite a length of 200 cm, a coiling of 2 cm diameter with adequate spacing in between each coil condenses this length into about 10 cm in height, which may easily fit into the insert. Second, despite this simple design the continuous heat exchanger has been found to be surprisingly effective. The tube of Wheatley, Rapp and Johnson reached a temperature of 26 mK at a molar flow rate of  $10^{-5}$  mol/s, well within the goal of under 100 mK.

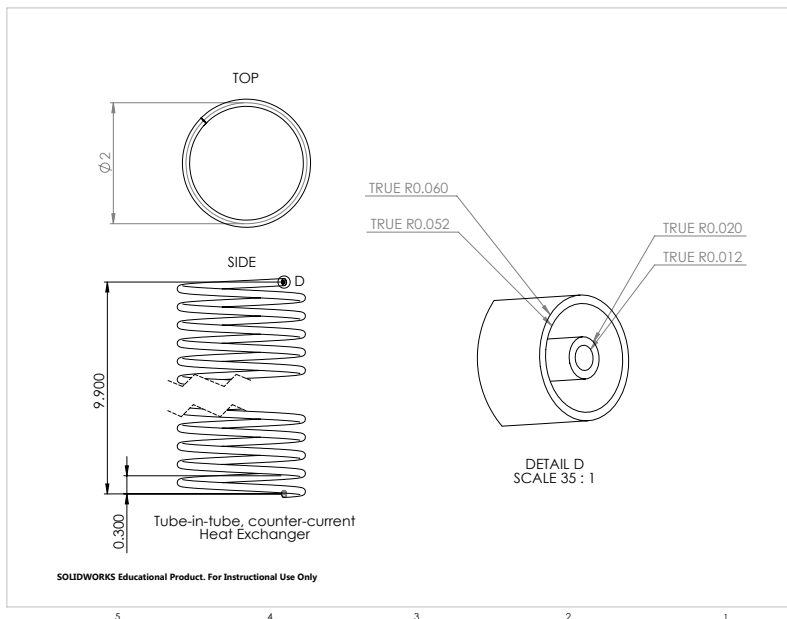


Figure 18: Main heat exchanger for the proposed dilution unit.

#### 4.4.7 Mixing Chamber

In the words of Frossati (1971), “[t]he particular design of a mixing chamber . . . does not seem to affect significantly the minimum temperature,” meaning that the size constraint presented does not affect the refrigerators ultimate performance. The mixing chamber may be made quite small, but as long as it houses a phase boundary, the fridge may continue cooling.

That being said, our situation is unique. For one, DNP requires microwaves be directly broadcast to the sample during experimentation. This poses a problem, as any thermal contact the mixing chamber has with the microwave line creates potential heat leaks to the mixing chamber, causing a decline in its performance. The solution to this problem proposed in this paper is the use of a crystal window atop the mixing chamber, through

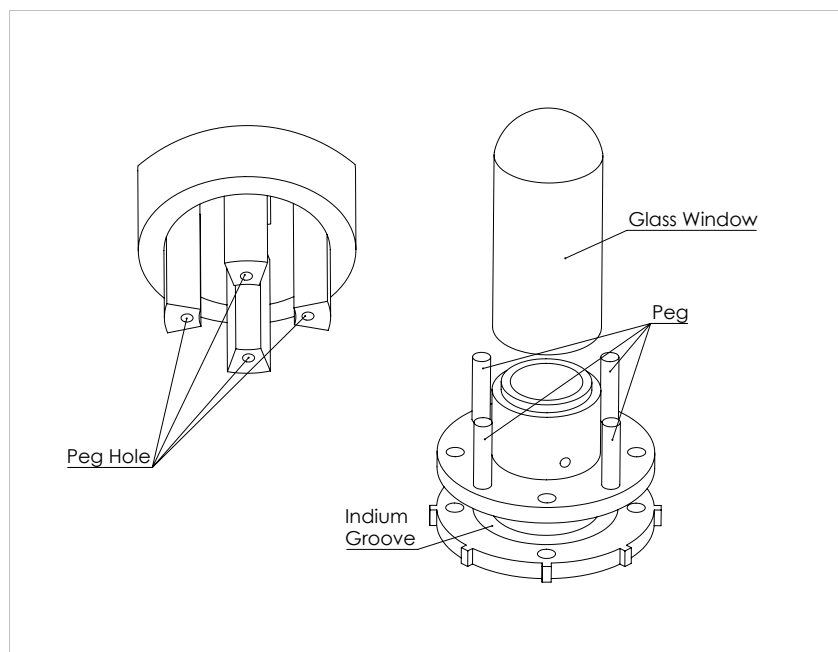


Figure 19: View of the mixing chamber (right) as well as the peg holds located on the graphite support (left). The mixing chamber will be made of copper and have an inner volume of about  $1 \text{ cm}^3$ .

which the microwaves may pass through into the mixing chamber and to the sample. This avoids any direct contact with the microwave line, while still allowing microwaves to the sample.

The mixing chamber is secured to the graphite support via fitted pegs that are wedged into peg holes. The mixing chamber is light enough for this connection to be secure enough for regular operation of the unit. Fig. 19 shows both the pegs on the mixing chamber as well as the peg holes of the graphite support.

Similar to the cap of the vacuum jacket, the mixing chamber cap has a groove for a 2mm thick ring of indium to provide a hermetic seal, as well as 2mm screw holes. Samples are loaded and unloaded by removing this cap, accessing inside the mixing chamber. It is desired that the torque from screwing/unscrewing at the mixing chamber cap won't damage the graphite to support to which it is attached. In order to do this, a scheme is devised in which the insert itself will be secured upside-down (so that the mixing chamber is toward the ceiling). The cap will be placed around a special "keyed" table so that when torque is supplied to tighten/loosen the screws, that torqued will be transferred to the table, and not the insert. In Fig. 19 this key shown in the form of small tabs on the cap, that would fit into some pre-made table for this purpose, although any shape would do.

## 5 Design Analysis

In designing the dilution insert, it is prudent to consider several different factors that are essential to operation: the heat load of the mixing chamber during operation, heat exchanger analysis, the pressure profile for the circulating  $^3\text{He}$ . While some design parameters may be adjustable, these must be explored and understood to confirm the possibility, and aid in the realization, of the dilution unit.

### 5.1 Heat Load of the Mixing Chamber

The heat load of the mixing chamber is extremely important to the operation of the dilution unit, as it is one of the factors that determine the minimum temperature achievable.

For the mixing chamber, heat load comes in three different varieties. First, the the mixing chamber must be initially cooled down from room temperature to 1 K, the temperature of the surrounding liquid Helium. Since the mixing chamber will initially contain a sample that needs to be kept at cryogenic temperatures, Sect. 5.1.1 is thus concerned with how much estimated time is need to cool down the metal of the mixing chamber. Sect. 5.1.2 looks at expected heat leaks to the mixing chamber during regular operation of the dilution refrigerator, with Sect. 5.1.3 dedicated to the heat load supplied by the microwaves sent down to the sample.

#### 5.1.1 Initial Heat Load

When the dilution unit is first inserted into the cryostat, the components of the fridge are first cooled down by the surrounding 1 K He. More specifically, heat is transferred from the innards of the dilution unit towards the 1 K plate and into the surrounding liquid He. An approximation of the time needed for this initial cool down is important since the sample placed within the mixing chamber must remain at cryogenic temperatures; it should be reasonable that heat leaves the innards of the fridge at such a rate so that the mixing chamber remains cold enough for the sample. In addition to this, the time required for cool down must also be practical for use in the lab.

A computer simulation was created to predict an approximate cool-down time. The innards of the fridge were treated as a one-dimensional bar with several sections of differing material, corresponding to the different components of the fridge. The design itself is discussed in Section 4, but a summary of the parts in order from top to bottom is as followed: 1 K plate (aluminum, 1 cm), graphite support (pitch-bonded graphite, 1.5 cm), still (aluminum, 9 cm), main graphite support (pitch-bonded graphite, 12 cm) and mixing chamber (copper, 3.2 cm). The 1-D bar was thus comprised of these subsections, spatially ordered as they were listed, with a total length of 26.7 cm.

Eq. 5 below is the usual 1D heat equation used to determine how heat is transferred over space and time. The temperature  $T$  of the 1D bar is determined by the thermal conductance  $k$ , density  $\rho$  and specific heat  $c$ . One underlying assumption of this equation

is that these values are constant with temperature. For the initial cool down, this isn't necessarily the case as the components are cooled from room temperature (approximately 300 K) down to cryogenic temperatures (around 1 K). Eq. 6 below takes these effects into account; a thorough derivation is provided in Appendix A.

$$\frac{\partial T}{\partial t} = \frac{k}{\rho c} \frac{\partial^2 T}{\partial x^2} \quad (5)$$

$$\rho c \frac{\partial T}{\partial t} = k \frac{\partial^2 T}{\partial x^2} + \frac{dk}{dT} \left( \frac{\partial T}{\partial x} \right)^2 \quad (6)$$

A computer simulation was created to numerically solve Eq. 6, over both time and space for given starting and boundary conditions. Data from various resources regarding the temperature dependence on thermal conductivity, heat capacity and density were gathered for copper, aluminum and pitch-bonded graphite to help accurately model the thermal properties of the bar [5] [6] [7] [8] [9] [10]. The entire bar was initially set to a temperature of 300 K with one end in contact with a reservoir of temperature 1 K (representing the point at which the 1 K plate touches the 1 K He when initially lowered into the cryostat) and the other end “insulated” so that heat only transferred through one end of the bar.

Fig. 20 shows the temperature profile of the dilution innards after ten minutes cool down. One prominent feature that may be noted is that the fridge begins cooling very quickly after first contact – within four minutes, the mixing chamber cools below 200 K. The 1 K plate cools very quickly, becoming 1 K almost immediately. The rest of the fridge fails to cool this quickly due to the graphite support between the 1 K plate and the still, and prevents these lower components from cooling more than approximately 90 K, even after several hours. The reason for this is due to the graphite support acting as a passive heat switch for the fridge. As explained in Section 4.4.5, pitch-bonded graphite was chosen as the connecting material between parts with differing temperature because it has a high thermal conductivity at high (room) temperatures and low thermal conductivity at low (cryogenic) temperatures. In theory, this allows heat to flow out of the innards during the cooling process and prevents heat from flowing in during operation of the fridge. However, this simulation highlights the fact that when the graphite support connecting the 1 K plate and the still reaches a certain low temperature during cool down, further cooling is halted due to this specific feature.

Fortunately, the innards of the fridge rest at 90 K, near the 77 K needed for the samples. In practice, the initial cool down will most likely be aided by placing liquid nitrogen in some components of the fridge (e.g. the mixing chamber), and so this quasi-steady state temperature would be more than adequate in experiment. Ultimately, this simulation predicts that passive cooling alone is nearly enough to keep the samples at cryogenic temperatures, leaving a difference that is easily overcome with liquid nitrogen pre-cooling techniques.

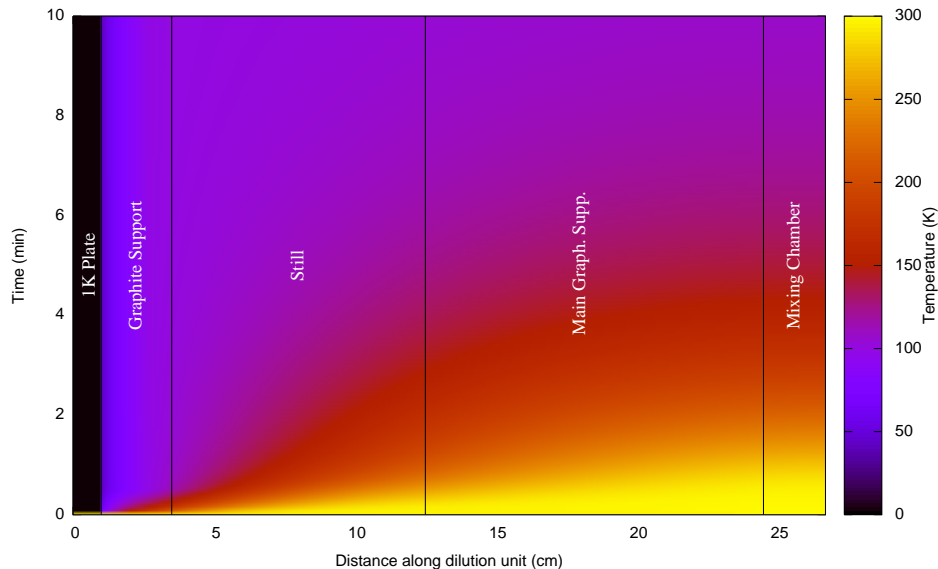


Figure 20: Temperature profile of the dilution fridge innards after ten minutes of cool down. Each portion of the dilution unit is marked on the figure.

### 5.1.2 Continuous Heat Leak

During continuous operation, heat leaks to the mixing chamber balance the cooling capacity of the fridge as it reaches its minimum temperature. The vacuum surrounding the mixing chamber is designed to minimize heat leaks between it the vacuum jacket, thus the biggest heat leak present during continuous operation would be heat transferred through the main graphite support. Using recent data on pitch-bonded graphite [9], the tube with dimensionality given in Sect. 4.4.5 would transmit approximately 25 nW of heat from a 0.7 K still to a 60 mK mixing chamber. This kind of heat load is more than manageable for the proposed fridge.

### 5.1.3 Microwave Heat Load

One concern for the mixing chamber is the heat load caused by the microwaves directly sent to the sample. It is estimated that this heat load be on the order of tens of micro Watts — three orders of magnitude more than a typical heat leak. The natural solution to this, looking at Eq. 2, would be to increase the molar flow rate in response. A high, although not unheard of, flow rate for this situation, then, could be  $10^{-4}$  mol/s or even  $10^{-3}$  mol/s. For example, a desired mixing chamber temperature of 50 mK and a heat load of  $20 \mu\text{W}$  will need a flow rate of  $10^{-4}$  mol/s to produce a reasonable result. If this heat load should rise to hundreds of micro Watts, then a molar flow rate of  $10^{-3}$  mol/s is more suitable.



While calculation is necessary to get an approximate idea of what is needed to cope with this heat load, it will most likely be experimentally-determined adjustments and experience with the fridge that will optimize the insert's DNP capabilities while reducing the microwave heat load when built.

## 5.2 Heat Exchanger Analysis

Much analysis has been done on continuous heat exchangers, both numerically and experimentally. In terms of mathematical analysis, Siegwarth and Radbaugh [4] classify a “good” continuous heat exchanger as one in which the heat transferred along the heat exchanger is small compared to the total heat transferred. In quantitative terms, they define this ratio in terms of the thermal conductance  $\kappa$ , cross-sectional area  $A$ , total length  $L$ , molar flow rate  $\dot{n}_3$  and molar specific heat  $c$ :

$$Y_i = \frac{\kappa_i A_i}{L_i \dot{n}_3 c_j}. \quad (7)$$

The subscript  $i$  may be  $c$ ,  $d$  or  $b$ , representing the column of liquid  $^3\text{He}$  contained within the inner tube, the column of dilute  $^4\text{He}$  in the annular space, and the body of the heat exchanger itself.

The total  $Y$  is the sum of these three ratios, and in order to be a suitable heat exchanger must be small in magnitude:

$$Y = \sum_i Y_i = \sum_i \frac{\kappa_i A_i}{L_i \dot{n}_3 c_j} \ll 1. \quad (8)$$

Once this is determined, Siegwarth and Radebaugh also provide a general differential equation to find the resulting temperature gradient along the heat exchanger. They assert that given a infinitesimal length of exchanger  $dx$ , there will be three main avenues of heat transfer: heat conduction along the heat exchanger by the established temperature gradient between the still and mixing chamber, Kapitza conduction between the dilute phase and concentrated phase, and viscous heat effects. All three of these contribute to the total change in enthalpy occurring in each section of the heat exchanger.

Suppose for a continuous heat exchanger that, in addition to the features above, also has a surface area of  $\sigma$  between the dilute and concentrated phase, a Kapitza resistance of  $\rho(T)$  (the inverse of which would be Kapitza conduction), and a temperature of  $T_b$ . Further suppose the liquid it carries has a viscosity value of  $\eta$ , molar volume of  $v_3$ , and flow impedance  $z$ . The following coupled differential equation then gives the temperature of either the dilute or concentrated side as:

$$A_i \underbrace{\left[ \kappa_i \frac{d^2 T_i}{dx^2} + \frac{d\kappa_i}{dT_i} \left( \frac{dT_i}{dx} \right)^2 \right]}_{\text{Heat conduction}} - \underbrace{\frac{d\sigma_i}{dx} \int_{T_b}^{T_i} \frac{dT}{\rho_i}}_{\text{Kaptiza conduction}} + \underbrace{\eta v_3^2 \dot{n}_3^2 \frac{dz}{dx}}_{\text{Viscous Heating}} = \underbrace{\dot{n}_3 c_i \frac{dT_i}{dx}}_{\text{Enthalpy change}} \quad (9)$$

Sect. 4.4.6 details a continuous heat exchanger built and tested by Wheatley, Rapp and Johnson [11]. With only about a meter of this type of heat exchanger, their dilution fridge was able to obtain a low temperature of 26 mK, well under the 100 mK goal.

The cupronickel describe by Wheatley was made of 70% copper and 30% nickel, which has a significantly lower thermal conductivity than other alloys, or even other cupronickel alloys with different proportions of each metal. Unfortunately, though, research has only been made on the transport properties of cupronickel material down to 4K, nowhere near the range desired. This 4K conductance, however, can still be taken as the *upper limit* on the actual conductance, as thermal conductance generally falls with decreasing temperature. Thus, we'll say  $\kappa_b \leq 0.0072$  (W/cm K) [12].

As for the  $c_b$ , Siegwarth explains that this value should be best given as the molar heat capacity of the dilute side, which has an upper limit of approximately  $75 \text{ J mol}^{-1} \text{ K}^{-1}$ .

Together, these values result in a maximum value for  $Y_b$  to be 0.005. This satisfies the condition placed by Eq. (8), meaning that this particular heat exchanger is ideal. The term in Eq. (9) due to heat conduction can then be ignored.

The Kaptiza resistance of the concentrated side for temperatures between .7K and .13K can be approximated as [13] :

$$\rho_c(T_c) = \left( \frac{2.4}{T_c^4} + \frac{1.55}{T_c^3} \right) \times 10^{-5} \quad [\text{cm}^2 \text{ K } \mu\text{W}^{-1}] \quad (10)$$

While at temperatures between .01 K and .13K, the following approximation is more appropriate:

$$\rho_c(T_c) = \left( \frac{20}{T_c^3} \right) \times 10^{-5} \quad [\text{cm}^2 \text{ K } \mu\text{W}^{-1}] \quad (11)$$

For the dilute side, its Kaptiza resistivity can be approximated over the entire temperature range with:

$$\rho_d(T_d) = \left( \frac{7}{T_d^3} \right) \times 10^{-5} \quad [\text{cm}^2 \text{ K } \mu\text{W}^{-1}] \quad (12)$$

Ignoring any viscous heating affects, all change in enthalpy, then, would be the cause of the Kapitza conduction; any heat leaving the concentrated side would (ideally) go directly into the dilute side, as shown below in Eq. (13) [13].

$$\frac{d\sigma_c}{dx} \int_{T_b}^{T_c} \frac{dT}{\rho_c} = \frac{d\sigma_d}{dx} \int_{T_d}^{T_b} \frac{dT}{\rho_d} \quad (13)$$

This integral can be solved numerically for  $T_b$  in terms of  $T_c$  and  $T_d$ , given the Kapitza conduction values for the concentrated and dilute side.

The value of  $\frac{d\sigma_i}{dx}$  for Wheatley's heat exchanger is simply  $2\pi r_i$ , where  $r_i$  is the radius of the inner tube that touches either the concentrated side ( $r_c = 0.32$  mm) or the dilute side ( $r_d = 0.4$  mm).

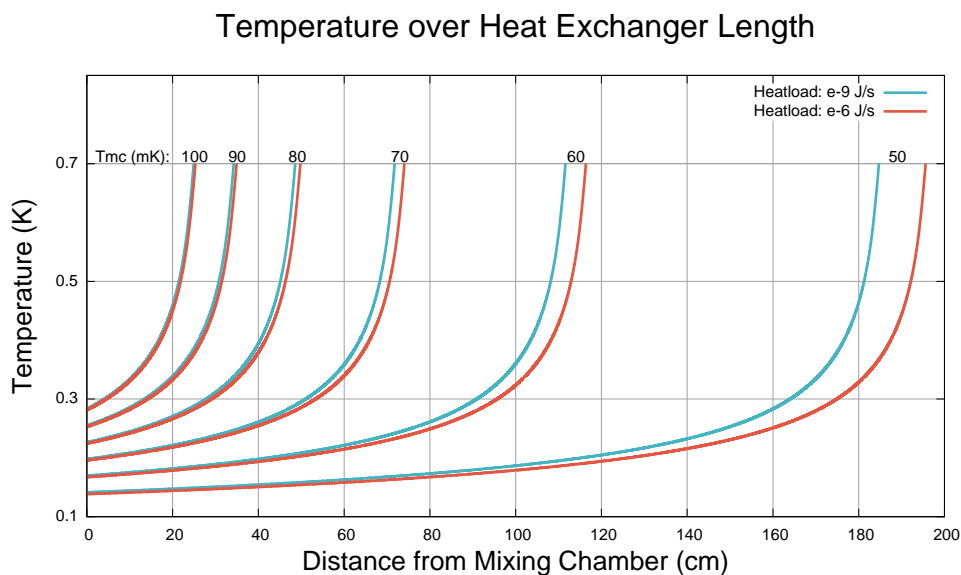
Simplifying Eq. (9) by ignoring the heat conduction and viscous heating terms, one can rearrange and reduce the expression to find the change in temperature per unit length:

$$\frac{dT_i}{dx} = -\frac{2\pi r_i}{\dot{n}_3 c_i} \int_{T_b}^{T_i} \frac{dT}{\rho_i} \quad (14)$$

A computer program using Eq. (14) was created to do simple analysis of sample heat exchanger lengths and heat loads. Taking as input the desired mixing chamber temperature, heat load and molar flowrate, Eq. 2 was used to find the temperature on the concentrated side necessary to match those conditions. These two temperatures —  $T_{mc}$  for the dilute side and  $T_c$  for the concentrated side — were the starting point for the program. From these values, Eq. (14) could be used by iteration to create a profile of the temperature as a function of distance from the mixing chamber.

Fig. 21 shows the resulting temperature profiles for several of these simulations. Keeping the flow rate of  $^3\text{He}$  at a constant  $10^{-4}$  mol/s across all simulations, mixing chamber temperatures of 100 mK down to 50 mK (as labeled on the graph) were tested against a heat load of  $\dot{Q} = 10^{-9}$  and  $10^{-6}$  W.

Figure 21: Temperature profile for several different heat exchanger situations.



Looking at Fig. 21, it is apparent how the Kapitza resistance becomes more of an issue at lower desired mixing chamber temperatures. For a heat load of  $10^{-6}$  W, a mere 25 cm of continuous heat exchanger is needed to reach 100 mK, while the same heat load requires nearly 2 meters for 50 mK. This may be somewhat surprising, but seems to reflect reality. For instance, in his proposal and experimentation of continuous heat exchangers, Wheatley states that from when it exits the still, the concentrated side lowers in temperature from 0.7 K to 0.3 K “within the first 10 cm...for [their] most successful heat exchanger” [11]. Using the above analysis method, .3 K is achieved over approximately 20 cm, reasonably agreeing with Wheatley’s observations.

Indeed, “surprisingly low temperatures can be reach in a dilution refrigerator equipped with a continuous exchanger only” [14]. The continuous heat exchanger of Wheatley, Rapp and Johnson (detailed above) achieved a minimum mixing chamber temperature of 26 mK with a molar flow rate of  $10^{-5}$  mol/s [11]. In general, Pobell suggests, a fridge whose minimum temperature is 40 mK only needs a single continuous heat exchanger of several meters in length [15].

Fig. 21 also suggests that a heat load of  $10^{-6}$  W or below is more than manageable for a heat exchanger of length 200 cm. Variations in heat load in this range also do not wildly impact the length of exchanger needed. For example, for a mixing chamber of 50 mK, an increase of heat load from  $10^{-9}$  W to  $10^{-6}$  W only requires a 10 cm extension of heat exchanger. Higher heat loads, however, become tricky. The reason for this is due to the limitations on the cooling power for a given molar flow rate. This can be seen by rearranging the change in enthalpy that occurs at the phase boundary Eq.(2), finding instead the temperature of the incoming  $^3\text{He}$  as a function of cooling power:

$$T_N = \sqrt{\frac{1}{12} \left( 96T_M^2 - \frac{\dot{Q}}{\dot{n}_3} \right)} \quad (15)$$

Because of the subtractive term under the square root, there is a point at which it is physically impossible to obtain a desired mixing chamber temperature for a given heat load. For a molar flow rate of  $10^{-4}$  mol/s and desired mixing chamber temperatures under 100 mK, this heat load starts to occur around tens of microWatts. Eq.(15) suggests that the only solution to a higher heat load is an increase in the circulation of  $^3\text{He}$ . This comes at a price, however, as the rate of temperature change along the heat exchanger, Eq.(14), is lowered by the raising of molar flow rate. Indeed, the effects are not trivial: for a heat load of 1 microWatt and a desired mixing chamber temperature of 100 mK, a flow rate of  $10^{-3}$  mol/s would need about 250 cm of heat exchanger - nearly ten times the length needed with a flow rate of  $10^{-4}$  mol/s. The strategy, then, should be to determine the minimum flow rate needed to achieve a desired mixing chamber temperature for the expected heat load, as this would also help determine the minimum length of heat exchanger needed.

This concern is not too prevalent in our purposes, as 100 nW of heat to the mixing chamber (while the microwave beam is turned off) is itself a very conservative estimation.

Nonetheless, it is good to keep these things in mind for any future experimentation of the cooling power of the dilution unit.

It may be noted that Fig. 21 neglects to include the dilute temperature profile. This is intentionally left out, as the dilute side doesn't significantly change in temperature for the majority of the heat exchanger's length due to its high specific heat. Only when the concentrated side nears .7 K does a slight rise in the dilution temperature occur.

### 5.3 Pressure Profile

Given that the pressure of the concentrated side is important to several points in the dilution fridge, it is prudent to consider the pressure and/or pressure drop at each point in the journey of the He<sup>3</sup>.

#### 5.3.1 Pressure Gradient Along a Circular Heat Exchanger

In his treatment of heat exchangers, White [18] gives an analytical method for finding the pressure gradient along a simple, continuous heat exchanger. Consider a pipe of diameter  $D$  (cm) and length  $L$  (cm), through which a fluid of molar mass  $M$  (g/mol), density  $\rho$  (g/cm<sup>-3</sup>) and viscosity  $\eta$  (poise) flows at a molar flow rate of  $\dot{n}$ . The pressure drop  $\Delta P$  that occurs due to viscous effects in the liquid as it travels across the length of the pipe is then given by the Darcy-Weisbach equation:

$$\Delta P = \frac{1}{2}\psi \frac{LG^2}{D\rho} \quad [\text{dyn cm}^{-2}] \quad (16)$$

Here, we define  $G$  as:

$$G = \frac{M\dot{n}}{\pi D^2} \quad (17)$$

$\psi$  is a dimensionless factor called the *Darcy Friction Factor*, and is dependent on the physical situation within the pipe, such as the shape and material of the pipe, as well as characteristics of the material flowing through it. It is usually dependent on the Reynolds number  $RE$  of the enclosed fluid (also dimensionless).

$$RE = \frac{GD}{\eta} \quad (18)$$

White explains for a circular tube, a Reynolds number of value less than 2300 corresponds to a regime of fluid flow called *laminar* flow, while RE values above this mark are considered to have *turbulent* flow. Laminar flow is characterized as high momentum diffusion and low momentum convection, i.e. the fluid is more-or-less well behaved as it moves from one end of the tube to another. Turbulent flow, as the name suggests, occurs when the flowing fluid is more sporadic and chaotic in nature, with a low momentum diffusion and high momentum convection.

For a circular pipe in the laminar flow regime, the Darcy Friction Factor is:

$$\psi_{lam} = \frac{64}{RE} \quad (19)$$

The Darcy Friction Factor for turbulent flow, on the other hand, is given by White as:

$$\psi_{turb} = 0.316(RE)^{-0.25} \quad (20)$$

### 5.3.2 Pertinent Properties of $^3\text{He}$

In order to use the above equations, it is necessary to determine some properties of liquid  $^3\text{He}$  as it travels towards the phase boundary; namely viscosity, molar mass and molar density.

Wheatley, Vilches and Abel [2] give the viscosity of the concentrated side as a "limiting low-temperature" value of:

$$\eta_c = (2 \times 10^{-6})/T^{-2} \quad [\text{poise}] \quad (21)$$

The molar mass of  $^3\text{He}$  is 3.02 g/mol, and its molar density can be approximated to be 0.08 g/cm<sup>-3</sup> for temperatures of under 1 K [16].

### 5.3.3 Tracing the Pressure Profile

In determining the desired pressure profile of the  $^3\text{He}$  as it travels towards the mixing chamber, it's best to start at the mixing chamber itself. At the phase boundary, zero pressure difference is wanted between the concentrated and dilute sides, since the phase boundary should be stationary within the mixing chamber (it is non-zero in the table below as this is the pressure needed from the incoming  $^3\text{He}$  to counteract the pressure of the dilution mixture also pushing against the phase boundary). A computer program incorporating the above equations was used to calculate the pressure experience by the  $^3\text{He}$  as it travels into the dilution unit and towards the mixing chamber. Care was taken to ensure pressures are high enough for the incoming  $^3\text{He}$  to condense as it approaches the 1 K plate, as well as stay condensed inside still (provided by a main and secondary impedance; see Sect. 4.4.2 and 4.4.4). Table [1] shows this pressure profile.

Table 1. Pressure profile of incoming  $^3\text{He}$ 

Part/Position	Pressure (torr)	Pressure Difference (torr)	Impedance Value ( $\text{cm}^{-3}$ )
Overhead Pressure	50	—	—
Primary Impedance	—	-38	$3.8 \times 10^{11}$
Still, Upper	12	—	—
Still Heat Exchanger	—	(negligible)	$5.83 \times 10^9$
Still, Lower	12	—	—
Secondary Impedance	—	-10.87	$1.1 \times 10^{11}$
Heat Exchanger, Upper	1.137	—	—
Heat Exchanger	—	-0.001	$1.94 \times 10^{10}$
Phase Boundary	1.136	—	—

## 6 Conclusion

In this paper, a design is proposed to use the cooling capabilities of a pre-existing helium cryostat as the starting point for a dilution refrigerator that would fit within the geometric constraints allowed by the cryostat. This cryostat already produces 1 K helium, an important first step for any dilution fridge. This new insert would provide the rest of the components necessary for dilution cooling (e.g. still, heat exchangers, mixing chamber), and thermally isolate these components from the 1 K helium into which this insert will be immersed.

Borrowing from over fifty years of dilution refrigeration research, this compact design also attempts to maximize overall performance while remaining within those geometric constraints. Two notable design aspects are the continuous heat exchanger that is compact yet reaches temperatures well under 100 mK, as well as the use of pitch-bonded graphite as a passive heat switch between temperature-sensitive components of the fridge.

The cooling power of the fridge is discussed, including potential sources of heat leak and heat load. The biggest concern for the insert is the heat load presented by the microwaves that are sent directly to the sample. With an estimated heat load on the order of 10  $\mu\text{W}$ , one solution proposed may be to increase the flow rate of  $^3\text{He}$  through the fridge, thereby increasing its cooling power. While these estimates provide a positive indication of the dilution units' ability to cope with this sort of heat load, experience with the fridge once it is built will most likely provide the best guidance.

Several mathematical analyses are also provided to model the performance of the proposed design. The initial cool-down of the insert is simulated, ensuring that the samples inserted into the mixing chamber remain at cryogenic temperatures. Temperature profiles of the proposed heat exchanger were calculated for different heat loads and mixing chamber temperatures, corroborating its experimentally suggested ability to provide enough heat exchange to allow adequate temperatures of the mixing chamber. The expected pressure profile of the dilution unit is also provided.

Possible next steps include analysis other key aspects of the dilution process, such as a thermodynamic analysis of the mixing chamber itself or a mathematical method for approximating rate of condensation at the condenser. As it stands, though, despite constraints imposed geometrically and by nature of the experiment involved, this paper gives much evidence in support of this design's ability to reach temperatures under 100 mK.



## References

- [1] Frossati, G. (1978)., Obtaining Ultralow Temperatures by Dilution of  $^3\text{He}$  into  $^4\text{He}$ , *Proc. 15<sup>th</sup> Int. Conf. on Low Temperature Physics*, Grenoble, France, 23 - 29 August 1978, in *J. de Physique, Colloque C-6, Suppl. no. 8*
- [2] Wheatley, J.C., Vilches, O.E., and Abel, W.R. *Phys.* **4** (1968)
- [3] Betts, D. S., *An Introduction to Millikevin Technology*, Cambridge University Press, New York (1989)
- [4] Radebaugh, R. and Siegwarth, J.D., *Cryogenics* **11** (1971)
- [5] White, G.K. and Collocott, S.J., *J. Phys. Chem. Ref. Data* **13** (1984)
- [6] Mendelssohn, K. and Rosenberg, H.M., *Proc. of the Phys. Soc. Section A* **65**, 6 (1952)
- [7] Jensen, J.E., Tuttle, W.A., Stewart, R.B., Brechna, H., Prodell, A.G., *Brookhaven National Laboratory Selected Cryogenic Data Notebook*, **1** (Brook Haven National Laboratory 1980)
- [8] Sheppard, R.G., Mathes, D.M., Bray, D.J., *Properties and Characteristics of Graphite for Industrial Applications* (POCO Graphite 2001)
- [9] Woodcraft, A.L., Barucci, M., Hastings, P.R., Lolli, L., Martelli, V., Risegari, L., Ventura, G., *Cryogenics* **49**, 5 (2009)
- [10] Hust, J.G. *A Fine-Grained, Isotropic Graphite for use as NBS Thermophysical Property RM's from 5 to 2500 K*, (National Bureau of Standards 1984)
- [11] Wheatly, J.C., Rapp, R.E. and Johnson, R.T., *J. Low Temperature Physics* **4** (1971)
- [12] Ho, C. Y., Ackerman, M. W., Wu, K. Y., Oh, S. G., Havill, T. N., *Thermal Conductivity of Ten Selected Binary Alloy Systems*
- [13] Siegwarth J.D., and Radebaugh, R. *The Review of Scientific Instruments* **Volume 42, Number 8** (1971)
- [14] Lounasmaa, O. V., *Experimental Principles and Methods Below 1 K*, Academic Press, New York (1974)
- [15] Pobell, F., *Matter and Methods at Low Temperatuers*, Springer-Verlag, Berlin (1994)
- [16] R.W.H. Webeler, D.C. Hammer, *Physics Letters*, **Volume 21, Issue 4**, June 1966, Pages 403-404
- [17] <https://userweb.jlab.org/~ckeith/TOOLS/HeVaporTable.html>

- [18] White, G.K., *Experimental Techniques in Low-Temperature Physics*, Stonebridge Press, Bristol (1968)

# Appendices

## A Heat Equation for Initial Heat Load

### A.1 Initial Formulation of the Equation

The rate of heat flow per unit area  $\vec{q}$  can be modeled in terms of the thermal conductivity  $k(T)$ , which is a function of temperature, and the gradient of the temperature  $\nabla T(\vec{r}, t)$ , where the temperature  $T$  is a function of both position and time. This relation is called Fourier's Law, which states that  $\vec{q}$  is in the same direction as this temperature gradient, and is proportional in value by  $k$ :

$$\vec{q} = -k\nabla T \quad (22)$$

The negative sign ensures that heat flows from areas of higher temperature to lower temperature (opposite the direction of the temperature gradient).

For a volume  $\Omega$ , the rate of change of internal energy of the volume  $\dot{Q}$  is simply the amount of heat leaving the boundary of the volume  $\delta\Omega$ . In terms of  $\vec{q}$ :

$$\begin{aligned} \dot{Q} &= - \iint_{\delta\Omega} \vec{q} \cdot \vec{d}\vec{a} \\ &= \iint_{\delta\Omega} k(T)\nabla T \cdot \vec{d}\vec{a} \\ &= \iiint_{\Omega} \nabla \cdot [k(T)\nabla T] dV \end{aligned} \quad (23)$$

where last step of Eq. (23) makes use of the Divergence theorem.

Care must be taken since the thermal conductivity is a function of temperature, and thus also has a dependence on position (and time), meaning it cannot be simply taken as constant. The integrand may be expanded out as

$$\begin{aligned} \nabla \cdot [k\nabla T] &= k\nabla^2 T + \nabla T \cdot \nabla k[T(\vec{r})] \\ &= k\nabla^2 T + \nabla T \cdot \left[ \frac{dk}{dT} \nabla T \right] \\ &= k\nabla^2 T + \frac{dk}{dT} (\nabla T)^2 \end{aligned}$$

Substitution of this expanded term into Eq. (23) results in

$$\dot{Q} = \iiint_{\Omega} \left[ k\nabla^2 T + \frac{dk}{dT} (\nabla T)^2 \right] dV \quad (24)$$

Next, consider an object with mass  $m$  and specific heat  $c(T)$ , a function of temperature. Assuming zero internal energy when  $T = 0$  K, the total energy  $Q$  found within this mass at temperature  $T$  can be found by adding together the heat capacities  $C$  of the object from  $C(T = 0)$  to  $C(T)$ , multiplying by  $dT$  at each step:

$$\begin{aligned} Q(T) &= \int_0^T C(T') dT' \\ &= m \int_0^T c(T') dT' \\ &= m \left[ \int_0^{T_0} c(T') dT' + \int_{T_0}^T c(T') dT' \right] \end{aligned}$$

The last line splits up the integral between an intermediary temperature  $T_0$ , which is the lowest temperature that the system can achieve. Because of this, the leftmost integral constant, simplifying later analysis of the system. For our purposes, define  $T_0 = 1$  K.

Since the volume  $\Omega$  is comprised of many of small masses  $dm$ , then the total energy found within  $\Omega$ , with mass density  $\rho$  and total mass  $M$ , is simply

$$\begin{aligned} Q_\Omega(T) &= \int dQ(T) \\ &= \iiint_\Omega dm \left[ \int_0^{T_0} c(T') dT' + \int_{T_0}^T c(T') dT' \right] \\ &= \iiint_\Omega \rho \left[ \int_0^{T_0} c(T') dT' + \int_{T_0}^T c(T') dT' \right] dV \\ &= \left( \int_0^{T_0} c(T') dT' \right) \iiint_\Omega \rho dV + \iiint_\Omega \rho \left[ \int_{T_0}^T c(T') dT' \right] dV \\ &= M \int_0^{T_0} c(T') dT' + \iiint_\Omega \rho \left[ \int_{T_0}^T c(T') dT' \right] dV \\ &= Q_\Omega(T_0) + \iiint_\Omega \rho \left[ \int_{T_0}^T c(T') dT' \right] dV \end{aligned}$$

In the last expression, the leftmost term is the total energy of the system at  $T = T_0$ . Since the system cannot go below  $T_0$ , this then is the lower energy limit of the system.

Differentiating this with respect to time:

$$\dot{Q}_\Omega = \iiint_\Omega \frac{\partial}{\partial t} \left\{ \rho \left[ \int_{T_0}^T c(T') dT' \right] \right\} dV \quad (25)$$

Notice that the  $Q_\Omega(T_0)$  term vanishes, since it is independent of time. In fact, the only term in the volume integrand that is explicitly dependent on time is the upper limit  $T$  of

the temperature integral. Both the mass density and the specific heat are dependent on temperature, so they are implicitly dependent on time as well.

Looking at the integrand of the volume integral, it can be expanded using product and chain rule:

$$\begin{aligned}\frac{\partial}{\partial t} \left\{ \rho \int_{T_0}^T c(T') dT' \right\} &= \frac{\partial \rho}{\partial t} \int_{T_0}^T c(T') dT' + \rho \frac{\partial}{\partial t} \int_{T_0}^T c(T') dT' \\ &= \frac{d\rho}{dT} \frac{\partial T}{\partial t} \int_{T_0}^T c(T') dT' + \rho \frac{\partial}{\partial t} \int_{T_0}^T c(T') dT'\end{aligned}$$

The rightmost term of the last line contains the time derivative of an integral, where as said before the only (explicit) dependence on time is the upper limit of the integral. In order to further reduce this expression, suppose that the specific heat function  $c(T')$  has an antiderivative that will be denoted as  $\zeta(T')$ . Thus the integral can be evaluated and simplified through the use of this antiderivative:

$$\begin{aligned}\frac{\partial}{\partial t} \int_{T_0}^T c(T') dT' &= \frac{\partial}{\partial t} [\zeta(T) - \zeta(T_0)] \\ &= \frac{\partial}{\partial t} \zeta(T) = \frac{\partial \zeta(T)}{\partial t} = \frac{d\zeta}{dT} \frac{\partial T}{\partial t} \\ &= c(T) \frac{\partial T}{\partial t}\end{aligned}$$

With this simplification, Eq. (25) may be written as

$$\dot{Q}_\Omega = \iiint_\Omega \left[ \rho c \frac{\partial T}{\partial t} \left( 1 + \frac{d\rho/dT}{\rho c} \int_{T_0}^T c(T') dT' \right) \right] dV \quad (26)$$

Both Eq. (24) and (26) describe the same physical quantity, the change in internal energy inside of  $\Omega$ . Since the domain of  $\Omega$  is arbitrary (i.e. the expression is true no matter what  $\Omega$  you choose), then the integrands must be equivalent:

$$\rho c \frac{\partial T}{\partial t} \left( 1 + \frac{d\rho/dT}{\rho c} \int_{T_0}^T c(T') dT' \right) = k \nabla^2 T + \frac{dk}{dT} (\nabla T)^2 \quad (27)$$

This is the general partial differential equation that describes temperature throughout a mass as a function of both position and time.

For our purposes, only one dimension of heat flow is necessary for analysis. In this case, Eq. (27) reduces down to

$$\rho c \frac{\partial T}{\partial t} \left( 1 + \frac{d\rho/dT}{\rho c} \int_{T_0}^T c(T') dT' \right) = k \frac{\partial^2 T}{\partial x^2} + \frac{dk}{dT} \left( \frac{\partial T}{\partial x} \right)^2 \quad (28)$$

If should be noted that if the density and thermal conductivity of a material are constant, then this expression can be further reduced down to

$$\frac{\partial T}{\partial t} = \frac{k}{\rho c} \frac{\partial^2 T}{\partial x^2}$$

$$\frac{\partial T}{\partial t} = \alpha \frac{\partial^2 T}{\partial x^2}$$

Which is the usual, second-order in space and first-order in time partial differential equation of temperature.

## A.2 Simplifying the Equation

In an attempt to simplify Eq.(28), consider the following term:

$$\frac{d\rho/dT}{\rho c} \int_{T_0}^T c(T') dT'$$

The change of density with respect to temperature can be expanded into, for an object with mass  $m$  and volume  $V$ :

$$\frac{\partial \rho}{\partial T} = \frac{\partial}{\partial T} \left( \frac{m}{V} \right) = -\frac{m}{V^2} \frac{dV}{dT}$$

The change in volume with respect to temperature is related to the coefficient of volumetric thermal expansion,  $\beta(T)$ :

$$\frac{dV}{dT} = V\beta(T)$$

The coefficient of volumetric thermal expansion may be approximated using the coefficient of *linear* expansion  $\alpha(T)$ , via the relation  $\beta \approx 3\alpha$ .

With this, the term in question can then be simplified to:

$$\chi(T) \equiv -\frac{3\alpha(T)}{c(T)} \int_{T_0}^T c(T') dT' \quad (29)$$

Examining this term in the context of Eq.(28), it may be entirely disregarded if  $\chi(T) \ll 1$  for all temperatures from 1 K to 300 K. For both aluminum and copper,  $\alpha$  and  $c$  were found over a temperature range of 1 K to 300 K, and  $\chi(T)$  calculated for temperature  $T$  along this range as well. It was found that  $\chi(T)$  never exceeded 0.02, satisfying this requirement. There is insufficient information on pitch-bonded graphite to do compute its highest  $\chi(T)$  value, but has similar linear expansion and heat-capacity measurements as both metals above (at least at room temperature), so it will be assumed that  $\chi(T)$  may also be ignored for the graphite as well.

### A.3 Final Heat-Equation Form

The above analysis allows Eq. (28), given the fridge's conditions, to be approximated as the following:

$$\rho c \frac{\partial T}{\partial t} = k \frac{\partial^2 T}{\partial x^2} + \frac{dk}{dT} \left( \frac{\partial T}{\partial x} \right)^2 \quad (30)$$